

Standard Title Page - Report on State Project

Report No. VTRC 06-CR12	Report Date April 2006	No. Pages 48	Type Report: Final Period Covered: October 2001 – April 2006	Project No.: 73977
				Contract No.
Title: Design of Bridging Layers in Geosynthetic-Reinforced, Column-Supported Embankments				Key Words: Column-supported embankment, bridging layer, geosynthetic-reinforced.
Authors: George M. Filz and Miriam E. Smith				
Performing Organization Name and Address: Virginia Transportation Research Council 530 Edgemont Road Charlottesville, VA 22903				
Sponsoring Agencies' Name and Address Virginia Department of Transportation 1401 E. Broad Street Richmond, VA 23219				
Supplementary Notes				
<p>Abstract</p> <p>The cost of column-supported embankments depends, in part, on the spacing between the columns and the size of the columns and pile caps. Geosynthetic reinforcement is often employed in bridging layers to enhance load transfer to the columns and to increase the column spacing. The number, stiffness, and strength of geosynthetic layers are selected based on considerations of load transfer and deformation.</p> <p>In this research, a new method was developed for calculating the load on the geosynthetic reinforcement. The new method employs one of the existing mechanistically based approaches and combines it with consideration of the stiffnesses of the embankment, geosynthetic reinforcement, columns, and existing site soil. The new method was verified against the results of a large numerical parameter study, for which the numerical procedures themselves were verified against closed-form solutions for membranes, pilot-scale experiments, and field case histories.</p> <p>The new method for calculating load on the geosynthetic was integrated into a 10-step design procedure for geosynthetic-reinforced bridging layers in column-supported embankments. The design procedure addresses such details as the thickness and type of the bridging layer soil, selection of the geosynthetic reinforcement, if needed, and the embankment settlement. The necessary calculations have been programmed into a Microsoft Excel® workbook. The workbook may be accessed at http://www.virginiadot.org/vtrc/main/online_reports/pdf/geogridbridge.htm.</p>				

FINAL CONTRACT REPORT

**DESIGN OF BRIDGING LAYERS IN GEOSYNTHETIC-REINFORCED,
COLUMN-SUPPORTED EMBANKMENTS**

George M. Filz
Professor
Via Department of Civil and Environmental Engineering
Virginia Polytechnic Institute & State University

Miriam E. Smith
Research Engineer
Swedish Geotechnical Institute

Project Manager
Edward J. Hoppe, Ph.D., P.E., Virginia Transportation Research Council

Contract Research Sponsored by the
Virginia Transportation Research Council

Virginia Transportation Research Council
(A partnership of the Virginia Department of Transportation
and the University of Virginia since 1948)

In Cooperation with the U.S. Department of Transportation
Federal Highway Administration

Charlottesville, Virginia

April 2006
VTRC 06-CR12

NOTICE

The project that is the subject of this report was done under contract for the Virginia Department of Transportation, Virginia Transportation Research Council. The contents of this report reflect the views of the authors, who are responsible for the facts and the accuracy of the data presented herein. The contents do not necessarily reflect the official views or policies of the Virginia Department of Transportation, the Commonwealth Transportation Board, or the Federal Highway Administration. This report does not constitute a standard, specification, or regulation.

Each contract report is peer reviewed and accepted for publication by Research Council staff with expertise in related technical areas. Final editing and proofreading of the report are performed by the contractor.

Copyright 2006 by the Commonwealth of Virginia.

ABSTRACT

Column-supported, geosynthetic-reinforced embankments have great potential for application in soft ground conditions, such as in coastal areas of Virginia, when there is a need to accelerate construction and/or protect adjacent facilities from the settlement that would otherwise be induced by the new embankment load. The columns in column-supported embankments can be driven piles, vibro-concrete columns, deep-mixing-method columns, stone columns, or any other suitable type of column. If driven piles are used, they are often fitted with pile caps to help transfer the embankment load to the piles. A bridging layer consisting of several feet of sand or sand and gravel is often used to help transfer the embankment load to the columns.

The cost of column-supported embankments depends, in part, on the spacing between the columns and the size of the columns or pile caps, if used. Geosynthetic reinforcement is often employed in bridging layers to enhance load transfer to the columns and increase the spacing between columns. The number, stiffness, and strength of geosynthetic layers are selected by geotechnical design engineers based on considerations of load transfer and deformations. Several methods to calculate the load on the geosynthetic reinforcement are described in the published literature, but the calculated loads differ by over an order of magnitude in some cases, and there is not agreement on which method is correct.

In this research, a new method was developed for calculating the load on the geosynthetic reinforcement. The new method employs one of the existing mechanistically based approaches, and combines it with consideration of the stiffnesses of the embankment, geosynthetic reinforcement, columns, and existing site soil. The new method was verified against the results of a large numerical parameter study, for which the numerical procedures themselves were verified against closed-form solutions for membranes, pilot-scale experiments, and field case histories.

The new method for calculating load on the geosynthetic was integrated into a 10-step design procedure for geosynthetic-reinforced bridging layers in column-supported embankments. The design procedure addresses such details as the thickness and type of the bridging layer soil, selection of the geosynthetic reinforcement, if needed, and the embankment settlement. The necessary calculations were programmed into a Microsoft Excel® workbook. The workbook may be accessed at http://www.virginiadot.org/vtrc/main/online_reports/pdf/geogridbridge.htm.

Both the numerical analyses and the simplified analysis procedure demonstrate the important impact that subgrade support has on the net vertical loads that are applied to geosynthetic reinforcement. If the subgrade support is good, like that provided by an existing near-surface layer of medium dense sand or stiff clay, and if the clear spacing between columns or pile caps is not too large, geosynthetic reinforcement does not have a significant effect on system performance. If the subgrade support is poor, like that provided by normally consolidated clay or peat, and if the clear spacing between columns or pile caps is large, it can become difficult to provide enough geosynthetic reinforcement to support the applied loads and limit deformations to acceptable magnitudes. In this case, it may be necessary to reduce the clear spacing between columns or pile caps. For appropriate column spacings and subgrade support conditions, geosynthetic reinforcement can enhance system performance.

FINAL CONTRACT REPORT

DESIGN OF BRIDGING LAYERS IN GEOSYNTHETIC-REINFORCED, COLUMN-SUPPORTED EMBANKMENTS

**George M. Filz
Professor**

**Via Department of Civil and Environmental Engineering
Virginia Polytechnic Institute & State University**

**Miriam E. Smith
Research Engineer
Swedish Geotechnical Institute**

INTRODUCTION

A research project entitled “Columnar Reinforcement of Soft Ground beneath Roadway Embankments” sponsored by the Virginia Transportation Research Council (VTRC) has generated two VTRC reports. This report addresses design of bridging layers in embankments supported on columns or piles, with or without pile caps. A later report will address the stability of column-supported embankments.

Geosynthetic-reinforced, column-supported embankments are constructed over soft ground to accelerate construction, improve embankment stability, control total and differential settlements, and protect adjacent facilities. The columns that extend into and through the soft ground can be of several different types: driven piles, vibro-concrete columns, deep-mixing-method columns, stone columns, etc. The columns are selected to be stiffer and stronger than the existing site soil, and if properly designed, they can prevent excessive movement of the embankment.

The columns are installed at a spacing determined by the design engineer, with lower costs for construction if the columns are widely spaced. A geosynthetic-reinforced bridging layer is often provided to transfer embankment and traffic loads to widely spaced columns. The bridging layer consists of several feet of compacted sand or sand and gravel, and it may include geosynthetic reinforcement. The geosynthetic reinforcement consists of one or more layers of planar polymeric material, which may be a woven geotextile or, more often, a geogrid.

Some authors attach special significance to the terminology used to refer to the bridging layer, which is also known as a load-transfer platform or a load-carrying geosynthetic layer, with the terminology used to imply specific mechanisms of load transfer from the embankment to the columns or pile caps. In this report, the term bridging layer is used in a generic sense without any intent to exclude valid mechanisms of load transfer.

Column-supported, geosynthetic-reinforced embankments are in widespread use in the United Kingdom, Scandinavia, and Japan, and they are becoming more common in the United

States and other countries. The column-supported, geosynthetic-reinforced embankment technology has potential application at many soft-ground sites, including coastal areas where existing embankments are being widened and new embankments are being constructed.

An alternative to column-supported embankments is use of prefabricated vertical drains combined with gradual placement of the embankment fill. This well-established technique can permit construction of embankments on soft ground at a lower construction cost than by using the column-supported, geosynthetic-reinforced embankment technology. However, use of vertical drains and gradual embankment placement may require considerable time for gradual consolidation and strengthening of the soft ground, and this approach can also induce settlement in adjacent facilities, such as would occur when an existing roadway embankment is being widened. If accelerated construction is necessary, or if adjacent existing facilities need to be protected, then column-supported, geosynthetic-reinforced embankments may be an appropriate technical solution.

The cost of column-supported, geosynthetic-reinforced embankments depends on several design features, including the details of the geosynthetic-reinforced bridging layer. Geotechnical design engineers establish the thickness and quality of the bridging layer soil and the number and type of geosynthetic layers within the bridging layer based on considerations of load transfer in the bridging layer and settlement of the embankment. This report summarizes the results of a research project performed to address these issues. All the details of the research cannot be covered in this summary report, which instead describes the key findings and the procedures recommended for use by design engineers in practice. Additional information is available in Smith (2005).

PURPOSE AND SCOPE

The primary purpose of this research was to develop a set of consistent and reliable procedures that geotechnical engineers can use to design bridging layers in column-supported, geosynthetic-reinforced embankments. The specific issues addressed by this research are settlement and load transfer in the bridging layer. The findings related to settlement and bridging layers are applicable to a wide variety of column types.

The scope of this research included:

- A review of the pertinent world-wide literature on column-supported, geosynthetic-reinforced embankments.
- Numerical stress-strain analyses of closed-form solutions, pilot-scale laboratory experiments, and field cases histories.
- Numerical parameter studies.
- Development of simplified analysis procedures.

- Development of recommendations for design of bridging layers in column-supported, geosynthetic-reinforced embankments.

The scope of this report does not include the design of column-supported embankments for slope stability, which will be addressed in a later report.

METHODS

This section describes the methods and procedures used for the literature review, numerical stress-strain analyses, and development of analysis and design procedures.

Literature Review

The literature review was based on searches using Compendex®, Web of Science®, and other search engines, including those supported by the American Society of Civil Engineers, the Federal Highway Administration, and the Swedish Geotechnical Institute. The contents of relevant journals and conference proceedings were also surveyed. Altogether, about 250 literature sources were reviewed. A comprehensive bibliography is available upon request.

Numerical Stress-Strain and Limit Equilibrium Analysis

Numerical stress-strain analyses of load transfer and settlement were performed using FLAC (Itasca 2002a), FLAC3D (Itasca 2002b), and SAGE (Morrison et al. 1993, Bentler et al. 1999).

FLAC and FLAC3D are finite difference analysis programs that solve the equations of motion for deformable bodies under load. FLAC performs analyses of problems in two dimensions. In this research, FLAC was used to perform axisymmetric analyses of a unit cell within a column-supported embankment to investigate settlement and load-transfer behavior under long-term drained conditions. FLAC3D performs analyses of problems in three dimensions. FLAC3D was used in this research to analyze the same issues for which FLAC was used, but with the full three-dimensional geometry considered.

SAGE is a finite element analysis program for two dimensional problems. Like FLAC, SAGE was used in this research to perform axisymmetric analyses of a unit cell within a column supported embankment. The SAGE analyses served two purposes. First, the SAGE analyses provided a check on the FLAC analyses. Second, SAGE analyses were performed to investigate whether significant differences exist between drained and water-soil coupled consolidation analyses of load transfer in column-supported embankments.

After the numerical analysis procedures were verified against closed-form solutions, pilot-scale laboratory tests, and field case histories, parametric numerical analyses were performed to determine the impacts of geometry and material property values on system performance.

Development of Analysis and Design Procedures

Findings from the literature review, investigation of case histories, and numerical analyses were all used to develop recommended procedures for analysis and design of bridging layers in column-supported embankments. Procedures using simple calculations familiar to geotechnical engineers were employed.

To facilitate the design process, a step-by-step design procedure was developed. A Microsoft Excel® workbook was developed for performing the necessary calculations.

RESULTS

This section describes the results obtained from the literature review, the numerical stress-strain analyses, and development of analysis and design procedures.

Literature Review

Results obtained from the literature review are grouped in the following three topic categories: analysis methods for settlement of column-supported embankments, analysis methods for geosynthetics in bridging layers, and general characteristics of column-supported embankments.

Analysis Methods for Settlement of Column-Supported Embankments

For embankments supported on driven piles or drilled shafts, the embankment settlement can be calculated by assuming that all of the embankment load is carried by the piles or drilled shafts and using established procedures for calculating settlement of deep foundation systems. Methods for calculating the settlement of driven pile and drilled shaft foundation systems are described by Hannigan et al. (1997) and O'Neill and Reese (1999), among others.

For embankments supported on deep-mixing-method columns, the settlement magnitude is determined by assuming equal strains for both the soft clay and the stiff column (Broms 1999, CDIT 2002, EuroSoilStab 2002). Equal strains are achieved by assuming that the vertical stress increments from the embankment and surcharge on the columns and the soil between columns are applied in the same proportion as the value of Young's modulus of the column, E_{col} , is to the value of the constrained modulus of the soil, M_{soil} . The implicit assumptions behind using E_{col} and M_{soil} are that a stiff column is not significantly restrained from lateral expansion by the soft soil but that the overall system geometry does provide lateral restraint for the soft soil in a unit cell. For columns installed by the deep mixing method, the modulus evaluated at 50% of the unconfined compressive strength, E_{50} , is often used for E_{col} .

Broms (1991) presents a load-spread method for calculating the compression of strata beneath columns installed by the deep mixing method.

Procedures for calculating settlement of embankments and structures supported on stone columns are described by Barksdale and Bachus (1983) and Pribe (1995). These procedures are summarized in an appendix of the dissertation by Smith (2005).

Russell et al. (2003) present a straight-forward method for including the effect of compliance at the base of the embankment on overall embankment settlement. In this approach, the volume of the differential settlement depression of the soft soil between the columns is distributed across the embankment to calculate a settlement component at the embankment surface. This approach is thought to be conservative because it does not consider expansion of the embankment soil that may occur due to dilatancy and reduction in normal stress above the foundation soil as consolidation proceeds.

Analysis Methods for Geosynthetics in Bridging Layers

Analysis methods have been published for vertical pressure acting on, as well as the resulting strain and tension developing in, geosynthetic reinforcement in bridging layers at the base of column-supported embankments.

Vertical Loads Acting on Geosynthetics in Bridging Layers

Several published methods for calculating the vertical loads applied by embankments and surcharges to geosynthetic reinforcement in bridging layers are briefly discussed and compared here. More details, including equations for all of the methods, are presented in Smith (2005). In all cases, the load on the geosynthetic can be expressed in terms of the stress reduction ratio, *SRR*, which is defined as the average stress on the subgrade soil or geosynthetic reinforcement spanning between columns to the average vertical stress at the base of the embankment due to the embankment weight plus surcharge. That is, $SRR = \sigma_{soil} / (\gamma H + q)$, where σ_{soil} is the stress on the soil between columns or pile caps, γ is the unit weight of the embankment fill, H is the embankment height, and q is the surcharge pressure at the surface of the embankment. σ_{soil} is often used as the vertical stress on the geosynthetic for the purpose of calculating strains and tension in the geosynthetic. For some of the methods, the reaction of the soil below the geosynthetic is taken into account.

The British Standard “Code of practice for strengthened/reinforced soils and other fills” (British Standards Institution 1995) has adopted an empirical method developed by Jones et al. (1990), which is based on Martson’s equation for a positive projecting conduit. In the BS8006 Method, the stress concentration on the piles, and consequently the stress remaining to be carried by the geosynthetic, depends on the pile type and the pile support condition.

The Adapted Terzaghi Method was developed by Russell and Pierpoint (1997) by modifying Terzaghi’s arching analysis to account for the three dimensional shape of the settling soil mass in the embankment above the foundation soil between the columns. Russell and Pierpoint applied a lateral earth pressure coefficient of unity in their Adapted Terzaghi Method. Later, Russell et al. (2003) presented a modified version of this method in which the lateral earth pressure coefficient is taken to be 0.5 and the upper 20% of the embankment is treated as a surcharge pressure. Both changes increase the calculated load on the geosynthetic. The decision

to treat the upper 20% of the embankment as a surcharge is intended to reduce the potential for differential settlement at the embankment surface. Russell et al. (2003) also provide a method for including the supporting capacity of the soil between columns based on a total stress analysis of load transfer from the soil to the columns.

Hewlett and Randolph (1988) present a method based on a limit equilibrium analysis of a hemispherical domed region above the columns or pile caps. The critical failure location is at either the top of the column or the crown of the arch. Kempfert et al. (1997) adopted the Hewlett and Randolph (1988) approach, with a modification for low-height embankments and for inclusion of subgrade support based on bearing capacity analysis.

Kempfert et al. (2004) present a method based on lower bound plasticity theory, pilot-scale tests, and numerical analyses. Like the Hewlett and Randolph (1988) Method, Kempfert et al. (2004) consider a domed arch spanning between columns or pile caps. Kempfert et al. (2004) provide for subgrade support of the geosynthetic reinforcement through use of a modulus of subgrade reaction.

Guido et al. (1987) showed that inclusion of stiff geogrids in granular layers beneath spread footings can improve bearing capacity. According to Bell et al. (1994), a result of the work by Guido et al. (1987) is that the angle of load spread through the geogrid-reinforced cohesionless soil can conservatively be taken as 45 degrees. Bell et al. (1994) applied this finding to evaluate an embankment with two layers of geosynthetic reinforcement supported on vibro-concrete columns. Russell and Pierpoint (1997) adapted the approach used by Bell et al. (1994) to determine an *SRR* value based on a single layer of reinforcement at the base of an embankment fill. Russell and Pierpoint (1997) assumed that the geosynthetic reinforcement carries a pyramid of soil that is not supported by the piles, with the ridge lines of the pyramid at an angle of 45 degrees above the horizontal. The Russell and Pierpoint (1997) expression of *SRR* is termed the Adapted Guido Method in this report.

Collin (2004) describes a refinement of the Adapted Guido Method, using approaches similar to those described by Bell et al. (1994), Jenner et al. (1998), and Card and Carter (1995). In Collin's refinement of the Adapted Guido Method, the sides rather than the ridges of the pyramid are inclined at 45 degrees above the horizontal, and at least three layers of reinforcement are necessary within the pyramid.

Carlsson (1987) presents in Swedish a method for calculating the vertical pressure on geosynthetic reinforcement in bridging layers. This method is discussed in English by Rogbeck et al. (1998) and Horgan and Sarsby (2002). The Carlsson Method considers a wedge of soil whose cross-sectional area under the arching soil can be approximated by a wedge with an internal angle at the apex of the wedge equal to 30°. The Carlsson Method adopts a critical height approach such that any additional overburden above the top of the wedge is transferred directly to the columns. The critical height is 1.87 times the clear spacing between pile caps.

Several authors have demonstrated that existing methods of determining *SRR* values yield very different results (Russell and Pierpoint 1997, Kempton et al. 1998, Habib et al. 2002, Horgan and Sarsby 2002). Rogbeck et al. (1998) point out that the BS8006 Method is not

continuous, and Love and Milligan (2003) observed that the BS8006 Method does not satisfy vertical equilibrium. For high values of the ratio of pile cap width to pile spacing, the BS8006 Method can give negative values of *SRR*. Russell and Pierpoint (1997) found that the Hewlett and Randolph Method and the Adapted Terzaghi Method were the most consistent with the results of three-dimensional numerical analyses. It is important to note that the tests conducted by Guido et al. (1987) investigated the influence of geosynthetic reinforcement located under footings subjected to downward loads, and these tests did not incorporate any piles or columns in the foundation soil. Regarding adaptation of these tests to column-supported embankments, Love and Milligan (2003) point out that the column or pile cap reaction force acts on geosynthetic reinforcement in the bridging layer in the opposite directions from the load due to the overlying embankment soil; whereas, the footing loads in the laboratory tests conducted by Guido et al. (1987) operated in the same direction as the load from the overlying soil.

Table 1 provides values of *SRR* determined from the existing methods discussed above for ranges of values of *a/s* and *H/s*, where *a* = the pile cap width, *H* = the embankment height, and *s* = the center-to-center spacing of the piles in a square array. The results in Table 1 were obtained using non-yielding piles and a friction angle of 35 degrees for the embankment fill. The subgrade soil reaction stresses mentioned by Kempfert et al. (1997), Russell et al. (2003), and Kempfert et al. (2004) were not applied so that all methods could be compared on the same basis. For all of the methods, it can be seen that the *SRR* values decrease with increasing values of *a/s* and *H/s*, for the ranges of *a/s* and *H/s* studied. However, for a given geometry, the *SRR* values vary greatly from one method to the next. For example, in the case of *a/s* = 0.25 and *H/s* = 1.5, the *SRR* value from the BS8006 Method is almost 8 times that from the Adapted Guido Method. It can also be seen that the *SRR* value is more sensitive to variations in the *a/s* value for the BS8006 Method than for any of the other methods. The Adapted Guido Method generally gives very low values of *SRR* compared to the other methods.

Table 1. *SRR* Values from Seven Existing Methods

Method	<i>SRR</i>					
	<i>a/s</i> = 0.25		<i>a/s</i> = 0.333		<i>a/s</i> = 0.5	
	<i>H/s</i> = 1.5	<i>H/s</i> = 4	<i>H/s</i> = 1.5	<i>H/s</i> = 4	<i>H/s</i> = 1.5	<i>H/s</i> = 4
BS8006 (1995)	0.92	0.34	0.62	0.23	0.09	0.02
Adapted Terzaghi, $K_T = 1$	0.60	0.32	0.50	0.23	0.34	0.13
Adapted Terzaghi, $K_T = 0.5$	0.77	0.52	0.69	0.42	0.54	0.26
Kempfert et al. (2004)	0.55	0.46	0.43	0.34	0.23	0.15
Hewlett and Randolph (1988)	0.52	0.48	0.43	0.31	0.30	0.13
Adapted Guido	0.12	0.04	0.10	0.04	0.08	0.03
Carlsson (1987)	0.47	0.18	0.42	0.16	0.31	0.12

Strain and Tension in Geosynthetics in Bridging Layers Due to Vertical Loads

Most procedures for calculating the strain and tension that develops in geosynthetics in bridging layers due to the vertical stresses from embankments and surcharge pressure are based on parabolic deflection of the geosynthetic (BS8006 1995, John 1987, Russell, et al. 2003, Rogbeck et al. 1998). These procedures also assume that the vertical loads on the geosynthetic are transferred to the portion of geosynthetic that spans directly between adjacent columns.

The strain and tension are obtained by simultaneously satisfying vertical equilibrium and load-strain compatibility for the geosynthetic that spans directly between adjacent columns Lawson (1992).

John (1987) provides an exact solution to the strain for parabolic deformation. BS8006 (1995), Rogbeck et al. (1998), and Russell et al. (2003) provide close approximations to the strain for parabolic deformation.

It is important at this point to distinguish between the BS8006 (1995) method to determine the vertical loads acting *on* the geosynthetic reinforcement and the BS8006 (1995) method to determine the strain and tension *in* the geosynthetic reinforcement. As shown in the previous section, the BS8006 (1995) method for calculating the vertical load acting *on* the geosynthetic is highly variable, and it is generally not in close agreement with several other published methods. On the other hand, most published methods for calculating the strain and tension *in* the geosynthetic reinforcement are similar to the BS8005 (1995) method in that they assume a parabolic deflected shape and they transfer the vertical loads acting on the geosynthetic to the portion of the geosynthetic that spans directly between adjacent columns. Any appropriate method for determining the vertical load acting *on* the geosynthetic can be applied to the BS8006 (1995) method for calculating the strain and tension *in* the geosynthetic.

Many designers limit the geosynthetic strain to 5 or 6 percent, with an additional 2 percent strain allowed for creep over the design life of the structure (e.g., BS8006 1995, Rogbeck et al. 1998).

Russell et al. (2003) describe use of high strength geosynthetics to span directly between columns and lower strength geosynthetics to cover the entire embankment area so that the interior portion of the unit cell is covered only by the lower strength geosynthetic. Russell et al. (2003) provide separate methods to calculate the tension in the higher strength and lower strength geosynthetics.

Kempfert et al. (2004) do not assume a parabolic deflected shape. Instead, they use a theory of elastic embedded membranes to evaluate the strain and tension in the geosynthetic reinforcement. Their results are presented in the form of a dimensionless design chart. The tension in the geosynthetic is obtained by multiplying the strain by the geosynthetic stiffness.

General Characteristics of Column-Supported Embankments

To limit differential settlements at the embankment surface, the clear spacing between columns or pile caps should not be too large in comparison with the embankment height. BS8006 (1995) recommends that the embankment height should not be less than 0.7 times the clear spacing between adjacent pile caps for square pile caps in a square array. Rogbeck et al. (1998) recommend that the embankment height should be at least equal to the clear spacing between pile caps, and that the embankment should be at least three feet high. Collin (2004) recommends that the embankment height should be equal to or greater than the clear span between columns. Kempfert et al. (2004) recommend that the embankment height should not be less than 1.4 times the clear diagonal spacing between columns in a square array. Converting the

diagonal clear spacing to the clear spacing between adjacent columns in a square array, the Kempfert et al. (2004) recommendation for minimum embankment height is about the same as the Rogbeck et al. (1998) and Collin (2004) recommendations. Kempfert et al. (2004) also recommend that the diagonal clear spacing of columns in a square array not exceed 10 ft for static loads or 8 ft for heavy live loads. Collin (2004) recommends that the clear spacing between adjacent columns not be greater than 10 ft. Hewlett and Randolph (1988) recommend that embankment height should be at least twice the center-to-center column spacing, which is a much more conservative limitation than the others mentioned here.

Regarding area replacement ratio, Rogbeck et al. (1998) recommend that the area replacement ratio should be at least 10 percent. This is consistent with the lower limit of the trend line shown by Han and Gabr (2002) for case histories of geosynthetic-reinforced, column-supported embankments.

According to Rogbeck et al. (1998) and Kempfert et al. (2004), the geosynthetic reinforcement should be placed as low as possible in the bridging layer to achieve greatest effectiveness, but some distance above the columns or pile caps should be maintained to reduce the potential for damage to the geosynthetic at the edges of the columns or pile caps. Rogbeck et al. (1998) indicate that the geosynthetic should be 4 in. above pile caps, and Kempfert et al. (2004) indicate that the bottom layer of geosynthetic should not be more than 6 in. above columns or pile caps. Kempfert et al. (2004) also recommend that, at most, two layers of reinforcement be used and that the vertical distance between reinforcement layers should be in the range from 6 to 12 in.

Hewlett and Randolph (1988) recommend that well compacted fill with a friction angle of at least 30 degrees be used in the bridging layer. According to Collin (2004), select structural fill with a friction angle greater than or equal to 35 degrees should be used in the bridging layer. Kempfert et al. (2004) indicate that cohesionless fill with a friction angle of at least 30 degrees should be used, although low-cohesion fill is permitted but not preferred. Naughton (personal communication, 2006) indicates that practice in the UK varies, but that select granular fill is often used in a 0.25 m to 1 m thick layer surrounding the geosynthetic(s) and that the overlying portion of the embankment is generally constructed of good quality fill with low fines content and a minimum friction angle of 30 degrees.

Results of Numerical Stress-Strain Analyses

In this section, the results of analyses performed to verify material modeling and numerical analysis procedures are described first. Then the results of parametric numerical analyses performed to investigate load transfer issues are described.

Verification of Numerical Analysis Procedures

Because numerical analyses are sensitive to material modeling and numerical modeling issues, it is important that verification analyses be performed. It is also important that principles of mechanics be followed to avoid getting the right answers for the wrong reasons. In this

research, numerical analyses of closed-form solutions, pilot-scale tests, and case histories were performed to verify suitability of the methods employed.

Verification and mesh refinement studies were performed using the finite difference method as implemented in FLAC (Itasca 2002a) and FLAC3D (Itasca 2002b) for axisymmetric and 3D membranes subjected to a uniform pressure. The numerical results were in good agreement with the closed-form solutions given by Ugural (1999). These studies, which are presented in Smith (2005), show that membranes can be successfully represented in FLAC and FLAC3D using thin solid mesh zones with small aspect ratios. At least two rows of mesh zones should be used.

Kempfert et al. (2004) present the results of pilot-scale tests of a geosynthetic-reinforced, column-supported embankment. As described in Smith (2005), drained axisymmetric FLAC analyses were performed for these pilot-scale tests, and Figure 1 shows that the comparison between measured and calculated stresses is good.

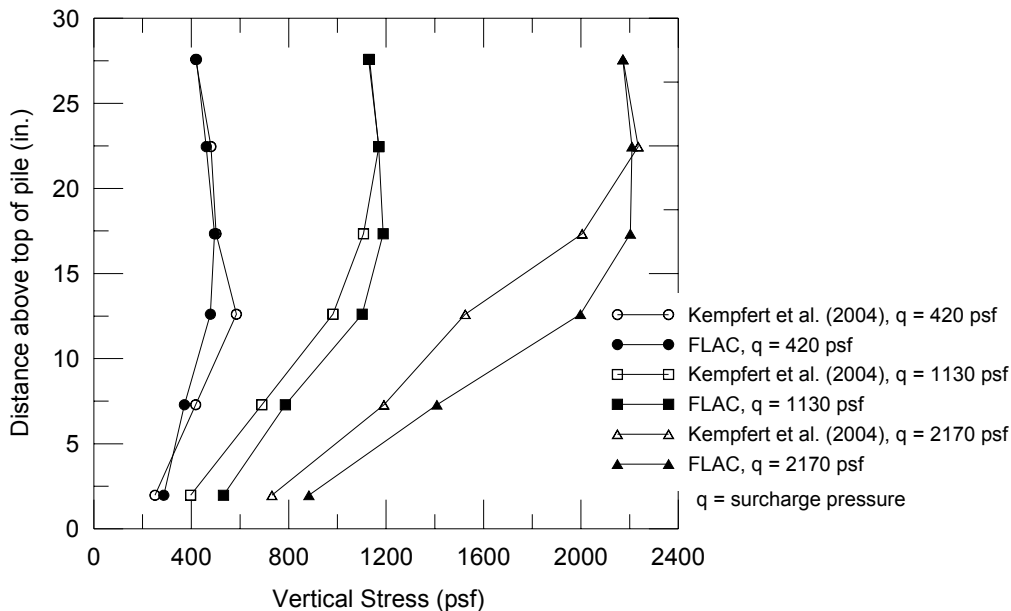


Figure 1. Comparison of axisymmetric FLAC drained analyses with pilot-scale test results reported by Kempfert et al. (2004).

The I-95/Route 1 test embankment is a well instrumented case of an embankment founded on columns installed by the dry method of deep mixing. The dry mix columns were 2.66 ft in diameter and installed in a triangular pattern at center-to-center spacings of 6 and 10 ft in two different regions beneath the embankment to produce area replacement ratios of 17.9% and 6.4%, respectively. The embankment was 18 ft high, and it was constructed with crushed aggregate after an initial placement of approximately 3 ft of bank run sand and gravel. One side of the test embankment consisted of a geosynthetic-reinforced retaining wall, and the other sides of the test embankment were constructed at 2H:1V slopes. Instrumentation included settlement plates, settlement pins, an observation well, vertical inclinometers, a horizontal inclinometer, vibrating-wire piezometers, magnetic extensometers, pressure cells, and thermistors. The test

embankment, as well as the material and numerical modeling details, is described in Stewart et al. (2004) and Smith (2005).

The results of drained, axisymmetric FLAC analyses are compared with readings from pressure cells in Figure 2. It can be seen that the agreement between measured and calculated response is good.

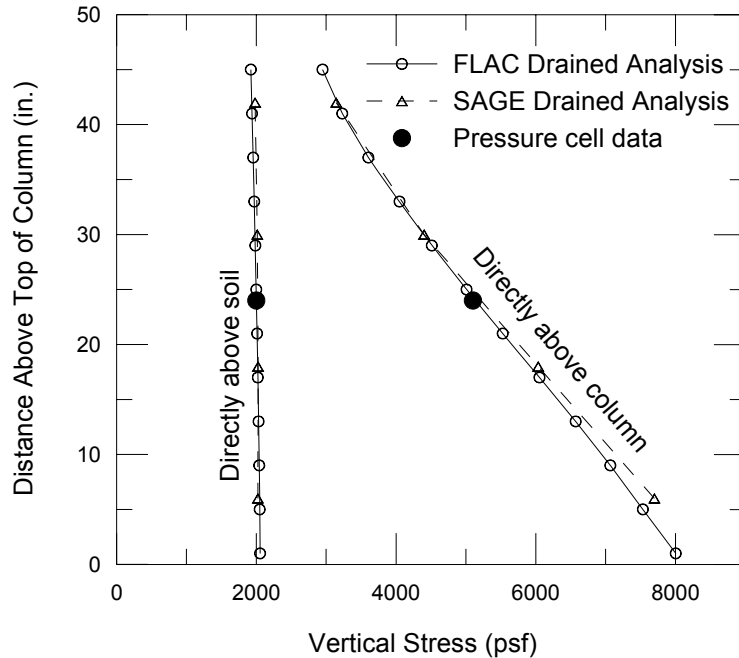


Figure 2. Measured and calculated vertical stresses at the I-95/Route 1 test embankment.

To verify the suitability of axisymmetric analyses for investigating load transfer issues in column-supported embankments, drained three-dimensional analyses were performed using FLAC3D. Figure 3 shows that the three-dimensional and two-dimensional analyses give virtually the same results. The two-dimensional axisymmetric results are smoother than the three-dimensional analysis results due to the greater mesh refinement that is possible in two-dimensional analyses.

To verify the suitability of drained analyses for investigating load transfer issues in column-supported embankments, axisymmetric consolidation analyses were performed for the I-95/Route 1 test embankment using the finite element analysis program SAGE (Morrison et al. 1993, Bentler et al. 1999), which provides efficient means for performing consolidation analyses. First, a drained analysis was performed using SAGE. The results of the SAGE drained analysis are compared to the results of the FLAC drained analysis in Figure 2, where it can be seen that the results are essentially the same. Next, a consolidation analysis was performed using SAGE. Figure 4 shows that the SAGE results are in good agreement with the time-rate of pressure development measured in the field. Furthermore, Figure 5 shows that the results of the SAGE analyses after completion of consolidation are in good agreement with the results of the SAGE drained analyses.

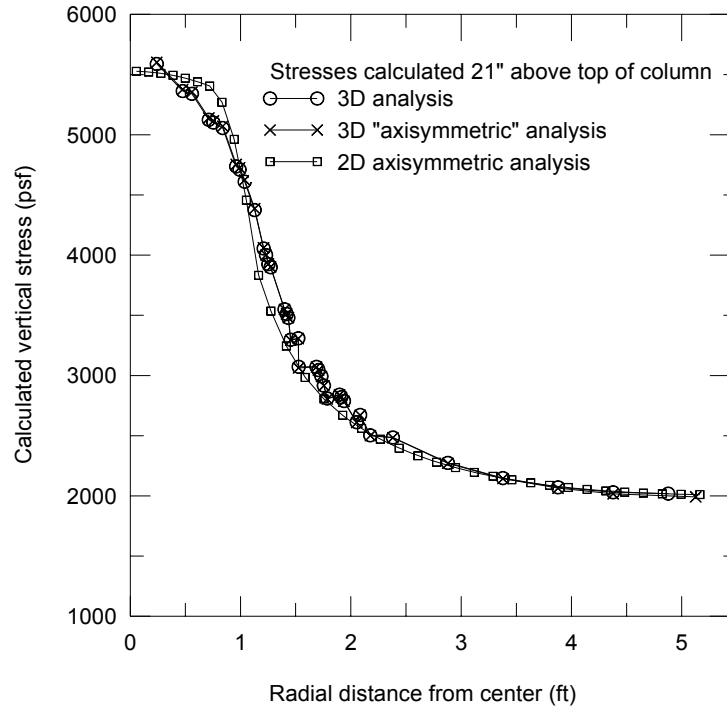


Figure 3. Comparison of two- and three-dimensional numerical analyses of the I-95/Route 1 test embankment at an elevation near the level of the pressure cells.

Numerical analyses were also performed for two additional case histories of geosynthetic-reinforced, column-supported embankments: the A14 and the Second Severn embankments described and analyzed by Russell and Pierpoint (1997). The axisymmetric FLAC analyses produced values of stress reduction ratio, *SRR*, that are in close agreement with the results of FLAC3D analyses by Russell and Pierpoint (1997) for the A14 embankment, but somewhat higher than the Russell and Pierpoint (1997) values for the Second Severn embankment. However, the axisymmetric FLAC results for the Second Severn embankment are in better agreement with the Adapted Terzaghi Method and the Hewlett and Randolph Method than are the FLAC3D results by Russell and Pierpoint (1997). Details of the axisymmetric FLAC analyses for the A14 and Second Severn embankments are in Smith (2005).

These verification studies show that drained axisymmetric FLAC analyses produce deflections and *SRR* values in good agreement with closed-form solutions, pilot-scale tests, and case histories.

Although properly performed axisymmetric analyses provide good representation of the average vertical stresses acting *on* geosynthetic reinforcement in bridging layers, axisymmetric analyses cannot be expected to provide realistic calculations of strain and tension *in* the geosynthetics because of (1) the orthotropic nature of geosynthetic reinforcement and (2) the possibility of stress concentrations at the corners of pile caps, if used. Either three-dimensional numerical analyses or a simplified representation of three-dimensional effects, like that in BS8006 (1995), should be used to calculate the strain and tension in the geosynthetic for the geometry of a column-supported embankment.

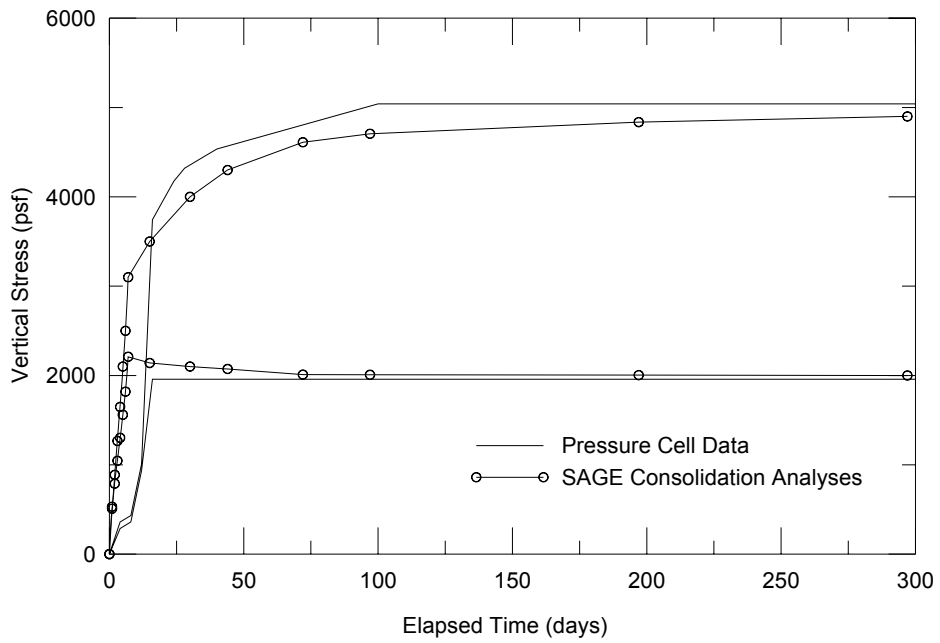


Figure 4. Comparison of numerical consolidation analyses with pressure cell data for the I-95/Route 1 test embankment.

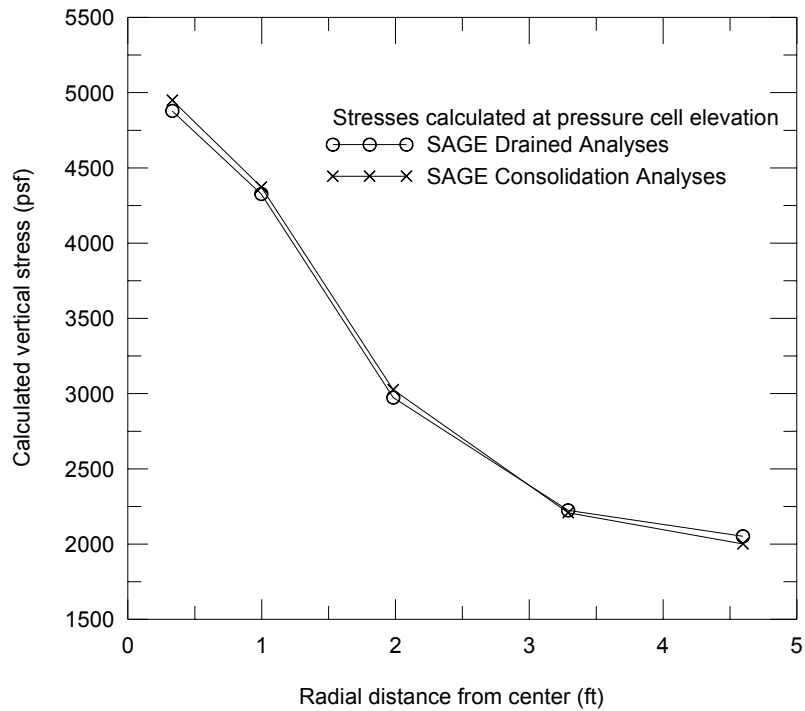


Figure 5. Comparison of axisymmetric SAGE drained and consolidation analyses.

Parametric Numerical Studies to Investigate Load Transfer Issues

Parametric numerical analyses were performed to identify and quantify the effects of factors that influence vertical load distribution among the column, geosynthetic reinforcement, and subgrade soil in column-supported embankments. The analyses were performed using FLAC with the material models and the drained axisymmetric analysis procedures that were verified against closed-form solutions, case histories, and pilot-scale experiments, as described above. Analyses were performed with and without geosynthetic reinforcement.

The parametric studies began with analysis of a base case, and then systematic variations of parameter values were applied. After the first round of analyses, additional cases of special interest were analyzed. The base case geometry for embankments without geosynthetic reinforcement in the bridging layer is shown in Figure 6, for which the column diameter and area replacement ratio are 2.68 ft and 20%, respectively. For embankments with geosynthetic reinforcement in the bridging layer, the base case column diameter and area replacement ratio are 2.3 ft and 10%, respectively, which corresponds to a larger column spacing than used for embankments without geosynthetic reinforcement. The base case material property values are shown in Table 2. The parameters that were varied and the range of varied parameter values are listed in Table 3. In addition to the variations listed in Table 3, the initial in-situ consolidation condition of the clay ranged from normally consolidated to 1000 psf above the initial in-situ vertical effective stress.

Table 2. Base case material property values

	Soft Clay	Upper Sand	Base Sand	Column	Embankment
Model type ^(a)	Modified Cam Clay	LEPP-MC	LEPP-MC	LEPP-MC	LEPP-MC
Moist density, lb/ft ³	-	115	-	= γ_{soil}	125
Sat. Density, lb/ft ³	96	120	140	= γ_{soil}	-
Elastic Modulus, psf	-	250,000	1,000,000	5,400,000	625,000
Poisson's Ratio	0.35	0.33	0.26	0.35	0.30
Bulk Modulus, psf	-	245,098	694,444	6,000,000	520,833
Shear Modulus, psf	-	93,985	396,825	2,000,000	240,835
q_u , psi	-	0	0	150	0
Friction Angle, deg.	-	30	40	0	35
Dilation Angle, deg.	-	0	0	0	0
Critical Shear Stress Ratio	1.1	-	-	-	-
Lambda, λ	0.35	-	-	-	-
Kappa, κ	0.035	-	-	-	-
Specific Volume, v_0	3.16	-	-	-	-
Pressure at v_0 , psf	100	-	-	-	-

(a) LEPP-MC: linear-elastic, perfectly plastic soil model with a Mohr-Coulomb failure criterion.

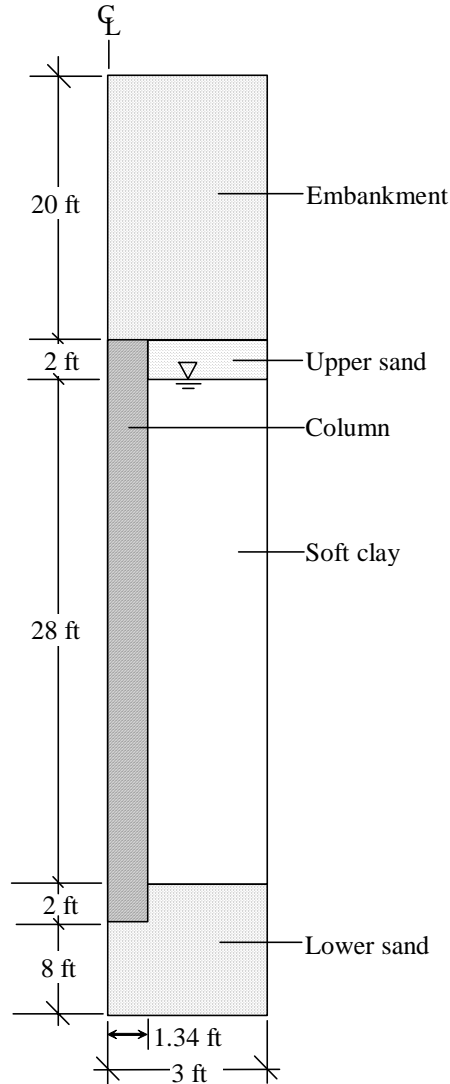


Figure 6. Base case axisymmetric geometry for numerical analyses.

The results of these parametric studies are described in detail in Smith (2005), and key findings are summarized here. One important result applicable to columns installed by the deep mixing method is that column failure occurred when the average embankment stress, $\gamma H + q$, divided by the area replacement ratio, a_s , was greater than about 90 percent of the unconfined compressive strength of the columns. This occurs due to stress concentration at the edges of the tops of the columns. The rest of the findings presented here are for column-supported embankments with columns that are strong enough to prevent column failure.

Table 3. Parameter variations used for numerical analyses

Item	Parameter	Range of Values
Embankment	Height	4 to 20 ft
	Unit Weight	115 to 135 psf
	Elastic Modulus	250,000 to 1,000,000 psf
	Poisson's Ratio	0.26 to 0.33
	Friction Angle	30 to 40 degrees
	Dilation Angle	0 to 10 degrees
Geosynthetic	Stiffness	8000 to 50,000 lb/ft
	Elevation above Columns	0 to 9 in.
Columns	Diameter	1.64 to 4.0 ft
	Area replacement ratio	0.05 to 0.40
	Unconfined Strength	30 to 700 psi
	Elastic Modulus	7,500 to 175,000 psi
Upper Sand Layer	Thickness	0 to 7 ft
Soft Clay	Thickness	18 to 38 ft
	Unit Weight	83 to 113 pcf
	Lambda	0.17 to 0.65
	Kappa	0.017 to 0.065
Lower Sand	Unit Weight	125 to 140 psf
	Elastic Modulus	625,000 to 2,000,000 psf
	Poisson's Ratio	0.23 to 0.3
	Friction Angle	35 to 45 degrees
	Dilation Angle	5 to 15 degrees

For embankments without geosynthetic reinforcement in the bridging layer, the findings are expressed in terms of the SRR_{fndn} value, which is the vertical stress on the subgrade soil between columns normalized by the average vertical stress from the embankment plus surcharge, $\gamma H + q$:

- SRR_{fndn} values decrease with increases in embankment height, embankment strength, embankment modulus, and column modulus.
- SRR_{fndn} values increase with increases in the thickness of the upper sand layer and modulus of the soft clay. However, these analyses showed that large changes in the modulus of the soft clay, such as would be produced by changing the clay from normally consolidated to overconsolidated, are needed to produce significant changes in SRR_{fndn} values.
- SRR_{fndn} values are unaffected, for practical purposes, by the thickness of the clay layer or the density of the lower sand. It is the subgrade soil conditions near the top of the columns that affect SRR_{fndn} values.
- SRR_{fndn} values are affected by column diameter and spacing in complex ways. For a fixed clear spacing between columns, SRR_{fndn} values tend to increase with increasing column diameter because there is decreasing stress concentration on the columns. For a fixed column diameter, as the clear span between columns increases, the upper sand and clay between columns is less able to span between columns, which tends to decrease SRR_{fndn} values, and the embankment is also less able to span across the

columns, which tends to increase SRR_{fndn} values. The net effect depends on the details of geometry and material property values.

These trends also apply for embankments with geosynthetic reinforcement in the bridging layer. The following additional findings are expressed in terms of the SRR_{net} value, which is the normalized difference between the vertical stresses on the top and bottom of the geosynthetic in the area not supported by columns. The normalization is by the average vertical stress from the embankment plus surcharge calculated at the elevation of the geosynthetic. SRR_{net} represents the net vertical stress on the geosynthetic, which is the stress that causes the geosynthetic to deflect downward and develop strain and tension.

- SRR_{net} values increase with increasing clear spacing between columns and increasing geosynthetic stiffness.
- SRR_{net} values decrease with increasing stiffness and strength of the foundation and embankment soils and with increasing elevation of the geosynthetic above the top of the columns or pile caps.

The quantitative results of these parametric numerical analyses are presented in Smith (2005). The quantitative results are also used below to show how the computational procedure recommended for design compares with the parametric numerical analyses.

Results of Development of Analysis and Design Procedures

In this section, the practical procedures that were developed for analysis and design of geosynthetic-reinforced bridging layers in column-supported embankments are described. These procedures are based on the results of the literature review and numerical analyses that were performed. First, calculation procedures for SRR_{net} , geosynthetic strain, geosynthetic tension, and embankment settlement are presented. Second, a comprehensive design procedure is described. Finally, the design and calculation procedures are illustrated with examples.

Calculation Procedures

A calculation model for the net vertical load acting on the geosynthetic was developed based on placing the geosynthetic reinforcement at the bottom of the embankment because this is the most effective location for the reinforcement (Rogbeck et al. 1998, Kempfert et al. 2004) and because this is a conservative location for calculating tension in the geosynthetic. In reality, the lowest layer of geosynthetic will be placed on a lift of granular material above the columns or pile caps to prevent local damage to the geosynthetic, and if more than one layer of geosynthetic is used, a lift of soil will be placed between adjacent layers of geosynthetic.

To begin, definition sketches are shown in Figures 7 and 8. Figure 7 shows pile caps laid out in plan view. A unit cell, which consists of one pile cap and the tributary soil defined by lines of symmetry, is also shown. For piles or columns laid out in a square array with center-to-center spacing, s , the area of the unit cell, A , is equal to s^2 . The area of the pile cap or column, A_c , is equal to a^2 or $\pi d_c^2/4$, where a = the width of a pile cap and d_c = the diameter of a column. The area of the tributary soil, A_s , is $A - A_c$. The area replacement ratio, a_s , is equal to A_c/A .

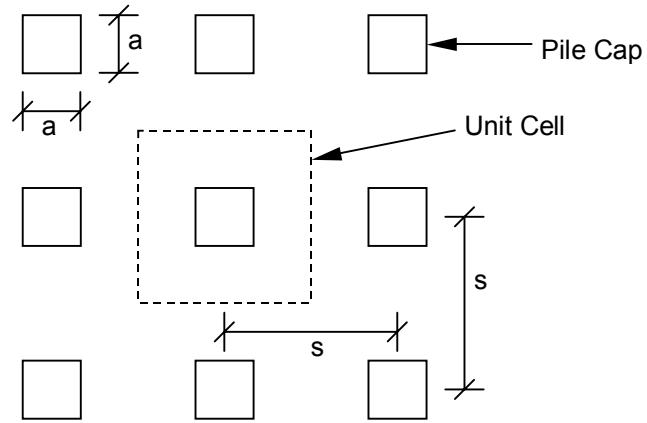


Figure 7. Definition sketch in plan view.

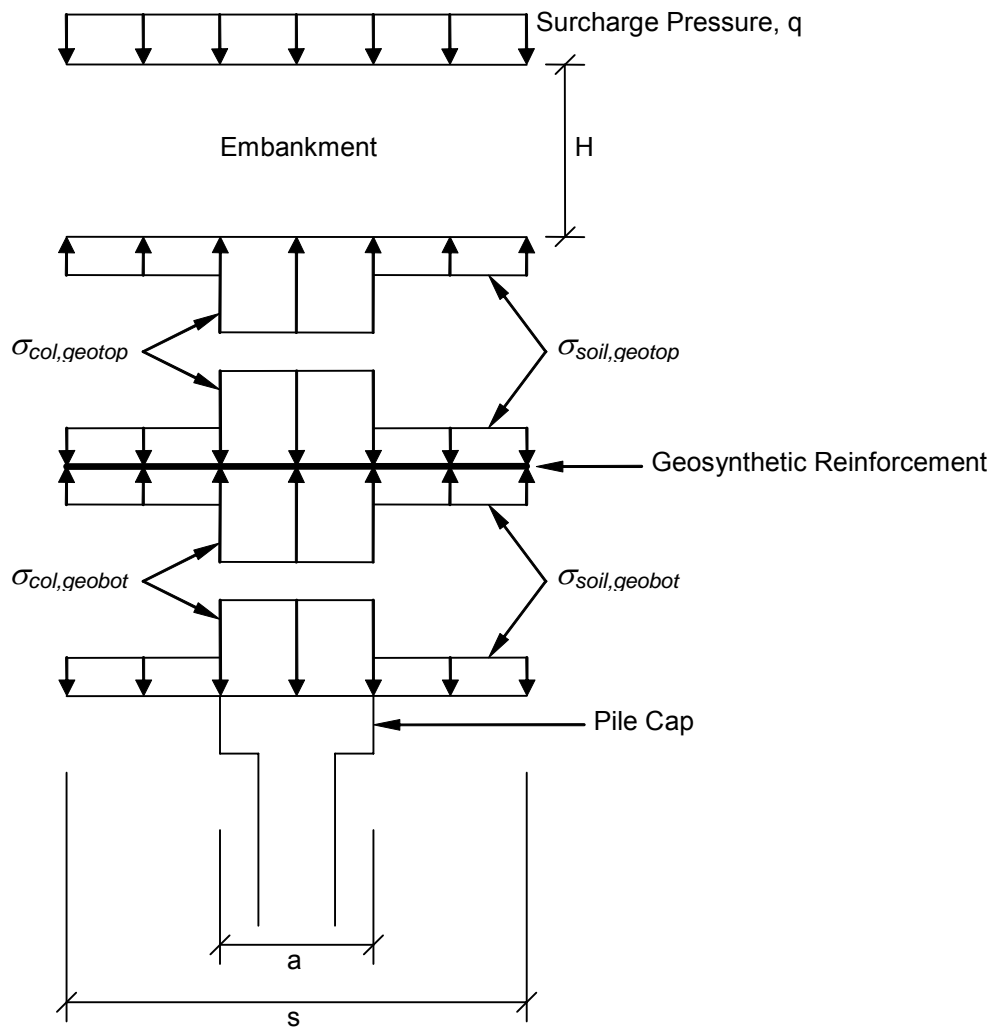


Figure 8. Definition sketch in profile view

Figure 8 shows an exploded profile view of a unit cell, including the vertical stresses at the contacts above and below the geosynthetic reinforcement. Values of stress reduction ratio applicable to the embankment, SRR_{emb} , the geogrid, SRR_{net} , and the foundation soil, SRR_{fndn} , are defined as follows:

$$SRR_{emb} = \frac{\sigma_{soil,geotop}}{\gamma H + q} \quad (1)$$

$$SRR_{net} = \frac{\sigma_{soil,geotop} - \sigma_{soil,geobot}}{\gamma H + q} \quad (2)$$

$$SRR_{fndn} = \frac{\sigma_{soil,geobot}}{\gamma H + q} \quad (3)$$

where $\sigma_{soil,geotop}$ = the vertical stress acting down on the top of the geosynthetic in the area underlain by the soil foundation and $\sigma_{soil,geobot}$ = the vertical stress acting up on the bottom of the geosynthetic in the area underlain by the soil foundation. From Eqs. (1) through (3), $SRR_{emb} = SRR_{net} + SRR_{fndn}$.

Vertical equilibrium requires that

$$\sigma_{col,geotop} = \frac{1 - (1 - a_s)SRR_{emb}}{a_s} (\gamma H + q) \quad (4)$$

$$\sigma_{col,geobot} = \frac{1 - (1 - a_s)SRR_{fndn}}{a_s} (\gamma H + q) \quad (5)$$

where $\sigma_{col,geotop}$ = the vertical stress acting down on the top of the geosynthetic in the area underlain by the column and $\sigma_{col,geobot}$ = the vertical stress acting up on the bottom of the geosynthetic in the area underlain by the column.

The procedures for obtaining the stresses on the embankment, geosynthetic reinforcement, column, and subgrade soil have several components, which are described here. First, the load-deflection relationship for the column or pile cap penetrating up, relatively, into the embankment is assumed to be linear up to the maximum load condition. The linear part is approximated using the linear-elastic solution for displacement of a circular loaded area on a semi-infinite mass, as provided by Poulos and Davis (1974). In the terms of this application,

$$d = \frac{\sqrt{\pi A_c} (1 - \nu_f) (\sigma_{col,geotop} - \sigma_{soil,geotop})}{2E_f} \quad (6)$$

where d = the relative displacement of the column or pile cap up into the embankment = the maximum differential settlement between the subgrade soil and the top of the column or pile cap, ν_f = the Poisson's ratio of the embankment fill, and E_f = the Young's modulus value of the embankment fill.

According to Eq. (6), at a relative displacement of $d = 0$, $\sigma_{col,geotop} = \sigma_{soil,geotop}$, which corresponds to $SRR_{emb} = 1$, as shown by combining Eqs. (1) and (4). With increasing relative displacement $d > 0$, $\sigma_{col,geotop} > \sigma_{soil,geotop}$, which corresponds to $SRR_{emb} < 1$.

The limiting stress condition in the embankment above the geosynthetic reinforcement is established by setting a lower limit on the value of SRR_{emb} using the Adapted Terzaghi Method:

$$SRR_{emb} \geq SRR_{lim} = \frac{\gamma}{\alpha(\gamma H + q)} (1 - e^{-\alpha H}) \quad (7)$$

where γ = the unit weight of the embankment fill, H = the embankment height, q = the surcharge pressure on top of the embankment, $\alpha = pK_T \tan(\phi)/A_s$, p = the column or pile cap perimeter, K_T = the lateral earth pressure coefficient in the embankment fill, ϕ = the friction angle of the embankment fill. The value of K_T is set equal to 0.75, which is between the values of 1.0 used by Russell and Pierpoint (1997) and 0.5 used by Russell et al. (2003). Eq. (7) can easily be adapted to embankments constructed of two types of fill material, as would occur when high quality soil is used in the bridging layer and lower quality soil is used above the bridging layer.

The Adapted Terzaghi Method was used to determine the limiting condition because this method is simple and it provided a reasonably good fit to the results of the verified numerical analyses, as shown below. However, other realistic methods for determining a limiting SRR value, such as the Hewlett and Randolph (1998) Method or the Kempfert et al. (2004) Method could be used in place of Eq. (7).

By combining Eqs. (1), (4), (6), and (7), the differential settlement at yield, d_{yield} , can be determined:

$$d_{yield} = \frac{\sqrt{\pi A_c} (1 - \nu_f) (1 - SRR_{lim}) (\gamma H + q)}{2a_s E_f} \quad (8)$$

According to this formulation, SRR_{emb} decreases linearly from a value of one at $d = 0$ to a value of SRR_{lim} at $d = d_{yield}$. For $d > d_{yield}$, SRR_{emb} remains at a value of SRR_{lim} .

The load-deflection response of the geosynthetic reinforcement was approximated by performing axisymmetric numerical analyses of a uniformly loaded annulus of membrane material with the inner boundary pinned, which represents the support provided by the column, and with the outer boundary free to move vertically but not laterally, which represents the axisymmetric approximation of lines of symmetry in the actual three-dimensional configuration of a column-supported embankment. The details of the analyses and the results are presented in Smith (2005). The results are closely approximated by the following expression:

$$d = \sqrt{\frac{A}{\pi}} \left[\frac{2}{3} \left(1 - \sqrt{a_s} + (1 - \sqrt{a_s})^4 \right) \sqrt[3]{\Sigma_g} + (1 - \sqrt{a_s})^3 \Sigma_g \right] \quad (9)$$

where d = the sag of the geosynthetic reinforcement = the maximum differential settlement between the subgrade soil and the top of the column or pile cap and Σ_g = the normalized vertical stress on the geosynthetic reinforcement, which is given by

$$\Sigma_g = \frac{(\sigma_{soil,geotop} - \sigma_{soil,geobot}) \sqrt{\frac{A}{\pi}}}{J_g} \quad (10)$$

where J_g = the stiffness of the geosynthetic reinforcement = $E_g t_g$, E_g = the modulus of the geosynthetic reinforcement, and t_g = the thickness of the geosynthetic reinforcement. Values of J_g can be obtained from tension tests on wide specimens or on single rib specimens, depending on the type of geosynthetic employed. The stress-strain response of many geosynthetics is nonlinear, and the stiffness value should be determined at an appropriate strain magnitude. If more than one layer of geosynthetic reinforcement is used, J_g should be set equal to the sum of the stiffnesses of the individual layers.

The settlements of the column and the subgrade soil are determined based on the vertical stress applied to the top of the column or pile, $\sigma_{col,geobot}$, and the vertical stress applied to the subgrade soil, $\sigma_{soil,geobot}$. As the soil settles down with respect to the column, the soil sheds load to the column through shear stresses at the contact between the soil and the column along the column perimeter. The magnitude of the shear stress, τ , is calculated using effective normal stresses:

$$\tau = \sigma'_h \tan \delta \quad (11)$$

where σ'_h = the effective lateral earth pressure at the soil-column contact and δ = the effective stress interface friction angle.

The value of σ'_h is determined from

$$\sigma'_h = K_0 \sigma'_{v,0} + \Delta \sigma'_h \quad (12)$$

where K_0 = the initial effective lateral earth pressure coefficient at the soil-column contact, $\sigma'_{v,0}$ = the initial vertical effective stress in the soil, and $\Delta \sigma'_h$ = the increment in the lateral effective stress at the soil-column contact due to the applied load.

The numerical analyses disclosed that the value of $\Delta \sigma'_h$ can be higher than would be expected based on one-dimensional compression of the soil because the column can bulge laterally in response to the applied load. This effect on $\Delta \sigma'_h$ values is most significant for portions of the column that are surrounded by sand. In the simplified calculation model, the value of $\Delta \sigma'_h$, as well as the vertical strain of the column and sand layers adjacent to the column,

are determined by using the solution for an elastic solid cylinder, which represents the column, surrounded by a concentric and laterally constrained thick-walled cylinder, which represents the soil. In the terms of this application, the relationships (after Poulos and Davis 1974) are:

$$\Delta\sigma'_h = \frac{v_{col}(1+a_s - v_{soil}(1-a_s))E_{soil}\Delta\sigma_{col} + v_{soil}(1+v_{soil})(1-a_s)E_{col}\Delta\sigma_{soil}}{(1-v_{col})(1+a_s - v_{soil}(1-a_s))E_{soil} + (1-v_{soil})^2(1-a_s)E_{col}} \quad (13)$$

$$\varepsilon_{col} = \frac{\Delta\sigma_{col} - 2v_{col}\Delta\sigma'_h}{E_{col}} \quad (14)$$

$$\varepsilon_{soil} = \frac{(1+v_{soil})[(1-2v_{soil}+a_s)\Delta\sigma_{soil} - 2a_s v_{soil}\Delta\sigma'_h]}{(1-v_{soil}+a_s(1+v_{soil}))E_{soil}} \quad (15)$$

where ε_{col} = the vertical strain in the column, v_{col} = the Poisson's ratio of the column, E_{col} = the Young's modulus of the column, $\Delta\sigma_{col}$ = the vertical stress increment in the column, ε_{soil} = the vertical strain in the soil, v_{soil} = the Poisson's ratio of the soil, E_{soil} = the Young's modulus of the soil, and $\Delta\sigma_{soil}$ = the vertical stress increment in the soil.

If the soil surrounding the column is clay instead of sand, the vertical strain in the soil is determined from:

$$\varepsilon_{soil} = C_{ec} \log \frac{p_0 + \Delta\sigma_{soil}}{p_0} \quad \text{for } p_0 = p_p \quad (16a)$$

$$\varepsilon_{soil} = C_{er} \log \frac{p_p}{p_0} + C_{ec} \log \frac{p_0 + \Delta\sigma_{soil}}{p_p} \quad \text{for } p_0 < p_p < p_0 + \Delta\sigma_{soil} \quad (16b)$$

$$\varepsilon_{soil} = C_{er} \log \frac{p_0 + \Delta\sigma_{soil}}{p_0} \quad \text{for } p_0 + \Delta\sigma_{soil} < p_p \quad (16c)$$

where C_{ec} = the compression ratio, C_{er} = the recompression ratio, p_0 = initial vertical effective stress, and p_p = preconsolidation pressure of the clay.

At the elevation of the top of the columns or pile caps, $\Delta\sigma_{col} = \sigma_{col,geobot}$ and $\Delta\sigma_{soil} = \sigma_{soil,geobot}$. As mentioned above, the value of $\Delta\sigma_{col}$ increases with depth and the value of $\Delta\sigma_{soil}$ decreases with depth due to load transfer from the soil to the column through the shear stresses around the column perimeter, as determined from Eq. (11). This process continues with depth until the column settlement and the soil settlement are equal. At and below this depth, the settlements and strains in the column and soil are equal. The compressions of the column and the soil between columns are determined by integrating the vertical strains in the column and the soil over the column length. The resulting soil compression represents the average compression of the soil between columns. In reality, the settlement profile of the subgrade soil at the level of the top of the columns is likely to be dish-shaped between columns. The difference between the

column compression and the average soil compression is the average differential settlement at subgrade level. To account for the dish-shaped settlement profile between columns, the suggestion of Russell et al. (2003) that the maximum differential settlement at subgrade level, d , may be as much as twice the average differential settlement was adopted.

The computational model described above is solved by satisfying vertical equilibrium and requiring that the calculated values of the maximum differential settlement at subgrade level, d , must be the same for the base of the embankment, the geosynthetic, and the underlying foundation soil.

A Microsoft Excel® workbook named GeogridBridge was developed to solve these equations and compute the value of SRR_{net} , which is then used to compute the strain and tension in the geosynthetic reinforcement, as described below. The workbook may be accessed at http://www.virginiadot.org/vtrc/main/online_reports/pdf/geogridbridge.htm. The workbook includes the following features:

- Two different types of embankment fill are allowed so that lower quality fill can be used above the bridging layer.
- Analyses without geosynthetic reinforcement can be performed by setting the value of J_g equal to zero.
- The column area and properties can vary with depth so that embankments supported on piles with pile caps can be analyzed.
- The subsurface profile can include two upper sand layers and two underlying clay layers. The preconsolidation pressure for the clay can vary linearly within each clay layer.

The spreadsheet was applied to the same cases analyzed in the numerical parameter study described above. Comparisons of the resulting SRR_{fndn} values for column-supported embankments without geosynthetic reinforcement and for SRR_{net} values for column-supported embankments with geosynthetic reinforcement are shown in Figure 9. It can be seen that the SRR_{net} values from the simplified theory tend to be greater than the SRR_{net} values from the FLAC analyses, which is conservative for strain and tension in the geosynthetic. The SRR_{fndn} values from the simplified theory tend to be less than the SRR_{fndn} values from the FLAC analyses, which is unconservative for calculating the settlement magnitude of column-supported embankments without geosynthetics; however, this is countered by the conservatism that is believed to exist in the Russell et al. (2003) procedure for estimating the component of embankment settlement due to embankment compliance, which is discussed here.

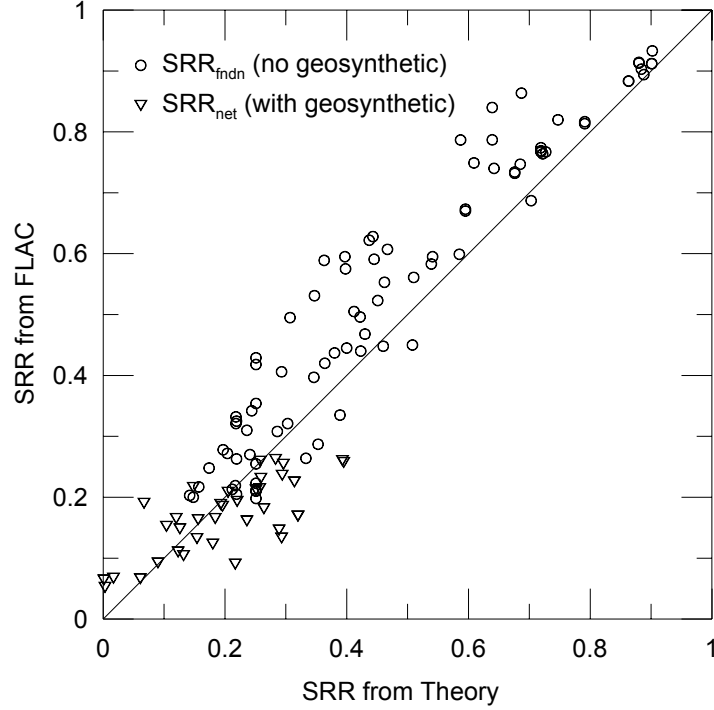


Figure 9. Comparison of SRR values from the simplified theory with SRR values from FLAC

For analysis of strain and tension in the geosynthetic reinforcement, the procedure presented in BS8006 (1995) is adopted. This is essentially the same procedure as employed by John (1987), Russell et al. (2003), Rogbeck et al. (1998), and others. In this approach, the load acting on the shaded area in Figure 10 is assumed to be carried by the portion of the geosynthetic reinforcement that spans directly between columns. This portion of the geosynthetic reinforcement is assumed to deform as a parabola. The strain in the geosynthetic reinforcement, ε_g , is obtained by solving the following cubic equation:

$$96\varepsilon_g^3 - 6K_g^2\varepsilon_g + K_g^2 = 0 \quad (17)$$

where $K_g = SRR_{net}(\gamma H + q)A_s/(J_g a)$, A_s = the area of tributary soil in a unit cell, and a = the pile cap width. If round columns or pile caps with diameter, d_c , are used, then the value of a is set equal to $0.886d_c$ when evaluating K_g .

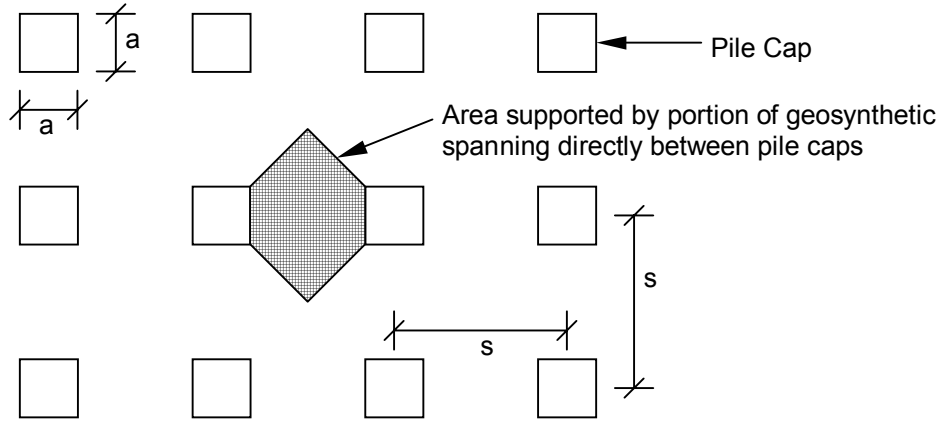


Figure 10. Area supported by geosynthetic spanning directly between columns.

The tension in the geosynthetic reinforcement, T_g , is obtained by multiplying the strain, ε_g , by the stiffness, J_g .

The GeogridBridge workbook solves Eq. (17) using the previously computed value of SRR_{net} to obtain values of strain and tension in the geosynthetic reinforcement.

The average total settlement, S , of the embankment is the sum of the embankment compliance, S_E , the compression of the columns, S_C , and the compression of underlying compressible material, S_U , if present:

$$S = S_E + S_C + S_U \quad (18)$$

The approach of Russell et al. (2003) can be used to account for compliance of the embankment at the level of the top of the columns. In this method, an approximation of the volume of the settlement dish between columns or pile caps is uniformly distributed to produce an increment of embankment settlement that is due to embankment compliance, S_E , according to

$$S_E = \frac{d(1 - a_s)}{2} \quad (19)$$

where d = the maximum differential settlement of the settlement dish between columns or pile caps computed as described above and a_s = the area replacement ratio.

The compression of the columns, S_C , is obtained by integrating the column strains, ε_{col} .

If compressible soil exists below the bottom of the columns, the load spread method described by Broms (1991) can be used to calculate compression of this underlying material, S_U . In this method, the embankment plus surcharge load is assumed to be carried down to the bottom of the columns, and then the load is distributed across an area that increases with depth at a rate of 1H:2V. Compression of the soil below the columns is computed using the resulting stress increments in the usual way.

Part of the embankment compliance settlement, S_E , occurs during construction as the differential settlement, d , develops in response to compression of soft soil near the original ground surface where the drainage path length is relatively short and significant consolidation occurs relatively quickly. From the point of view of the overlying pavement, the settlement and differential settlement of the embankment that occur as the embankment is placed and before the pavement section is constructed are not detrimental. Only the additional settlements that occur after pavement construction have the potential to damage the pavement. However, the entire differential settlement, d , that occurs at subgrade level is important for the geosynthetic reinforcement, and the foundation and embankment system should be designed to keep the geosynthetic strains and tensions within allowable limits.

Consolidation analyses can be performed to estimate the amount of compliance settlement that occurs prior to pavement construction. Janbu's (1963) method for consolidation of clay layers with non-uniform strain profiles is useful for these calculations because the ultimate strain profile that develops in the clay between columns due to the embankment load decreases with depth as the clay sheds load to the stiffer columns through shear stresses at the contact between the clay and the columns.

Consolidation analyses using Janbu's (1963) method with a linear strain profile are incorporated in the GeogridBridge workbook, with the user providing values of the time available for consolidation, t , and the coefficient of consolidation, c_v . The time available for consolidation, t , is the time between the mid-point of embankment construction and placement of the pavement, as shown in Figure 11(a), or the time between the mid-point of embankment plus preload construction and the mid-point of preload removal, as shown in Figure 11(b). In the GeogridBridge worksheet, a single value of c_v is used to characterize the time-rate of consolidation of the clay even if two layers of clay are present. The value of c_v should be selected with judgment considering the consolidation state of the clay layers and recognizing that most of the clay compression will occur in the upper portion of the clay deposit. The settlement that occurs during the consolidation period is subtracted from the total settlement to determine the average post-construction settlement of the pavement surface.

According to the published literature summarized previously, the differential settlement of the pavement surface between a location above a column or pile cap and a location above the existing site soil at the center of a unit cell should be small if the embankment height exceeds the clear spacing between columns or pile caps.

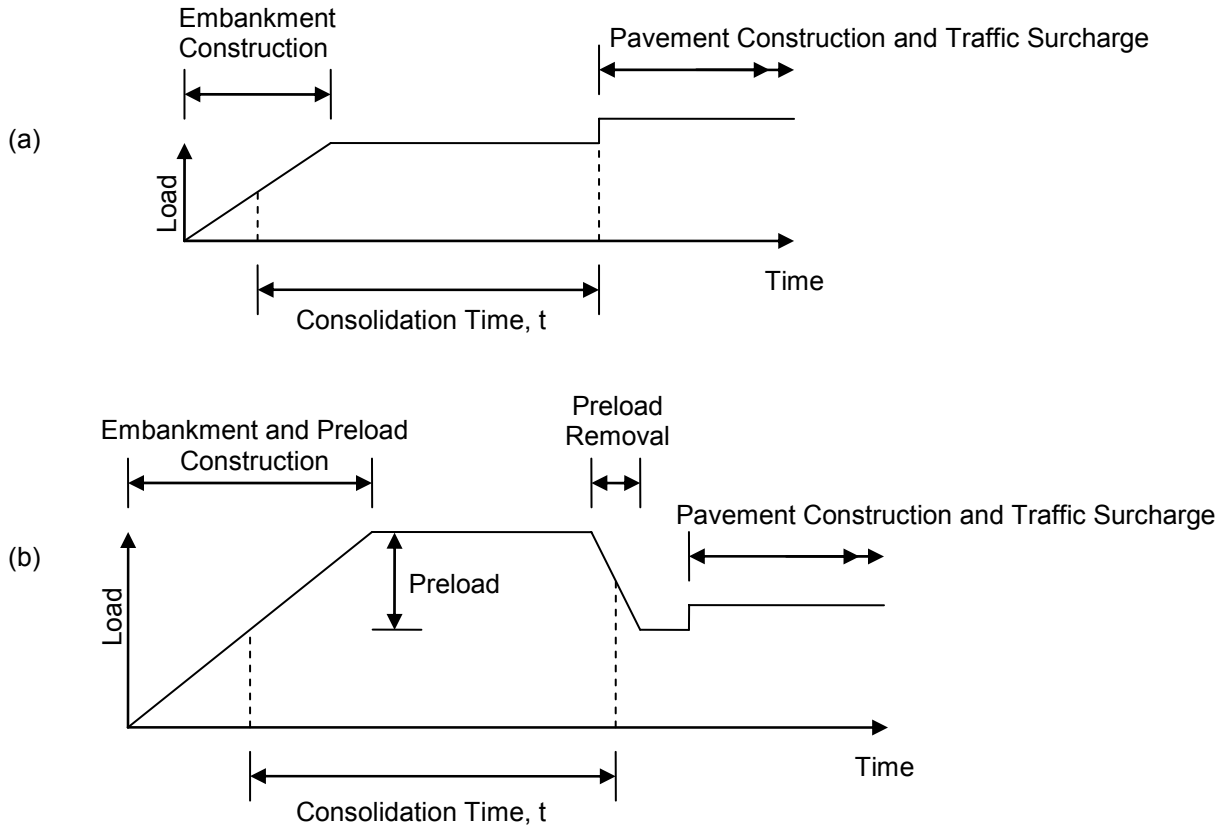


Figure 11. Time available for consolidation of an embankment constructed (a) without preload and (b) with preload.

Design Procedure

The following step-by-step procedure is recommended for design of geosynthetic-reinforced, column-supported embankments:

1. Collect project information, including the required embankment height, H , the pavement and traffic surcharge loading, q , and the maximum allowable post-construction embankment settlement, S .
2. Collect subsurface information, including stratigraphy, field test data, laboratory test results, and ground water information. Develop subsurface profile(s) for design.
3. Select trial values of the maximum center-to-center column spacing, s , of columns in a square array and the minimum column diameter, d_c , or pile cap width, a , to satisfy all three of the following criteria, which were obtained from a synthesis of recommendations in the literature:
 - a. $s - a \leq H$
 - b. $s - a \leq 8 \text{ ft}$
 - c. $a_s \geq 0.10$

If round columns of diameter, d_c , are used, then set a equal to $0.886d_c$ when applying criteria a. and b. The area replacement ratio, a_s , is given by a^2/s^2 or $\pi d_c^2/(4s^2)$. Regarding the criterion that the clear spacing between columns, $s - a$, should not exceed the embankment height, H , it is recognized that most problems with geosynthetic-reinforced, column-supported embankments have occurred with low-height embankments. Consequently, if $s - a$ approaches H , special care should be exercised to ensure that geosynthetic layers are properly placed without slack, that high quality and well compacted GW material is used for the bridging layer, and that a preload be considered to minimize post-construction differential settlements of pavements.

4. Select a clean sand or sand and gravel for the bridging layer. This should be an SP, SW, GW, or GP material, according to the Unified Soil Classification System. Estimate the values of unit weight, friction angle, modulus, and Poisson's ratio for this material. The thickness of the bridging layer fill, H_b , should satisfy both of the following criteria:
 - a. $H_b \geq 3$ ft
 - b. $H_b \geq s - a - H_{b,red}$, where $H_{b,red}$ is an amount that the bridging layer thickness can be reduced if an upper layer of strong soil exists at the site. The value of $H_{b,red}$ should be selected by the designer using conservative engineering judgment to reflect the bridging action that will occur in the competent surface layer. Suggested values of $H_{b,red}$ are one-third the thickness of an existing surface layer of loose sand and one-half the thickness of an existing surface layer of medium dense sand. The value of $H_{b,red}$ should never be greater than one-half the thickness of the competent surface layer. If poor ground, such as normally consolidated clay, peat, or very loose sand, extends to the original ground surface, then the value of $H_{b,red}$ should be set equal to zero.
5. Determine the embankment fill material that will be used above the bridging layer. This may be any suitable material for embankment construction. Estimate the values of unit weight, friction angle, modulus, and Poisson's ratio for this material.
6. Design the columns or piles to be able carry the entire load from the embankment and surcharge with an adequate factor of safety. Thus, each column should be designed to carry an allowable load of $(\gamma H + q)s^2$. Based on the results in Smith (2005), if the columns are deep-mixing-method columns, then the unconfined compressive strength of the columns should exceed $1.1(\gamma H + q)/a_s$ by a suitable factor of safety.
7. Select a suitable layer or layers of geosynthetic reinforcement. Between one and three layers of geosynthetic reinforcement can be used. The geosynthetic reinforcement is treated as a single layer in the GeogridBridge workbook, with the value of J_g set equal to the sum of the stiffnesses of the individual layers. The geosynthetic reinforcement should be selected to satisfy the following criteria, using the workbook to calculate the strain in the geosynthetic reinforcement, ε_g , and the tension in the geosynthetic reinforcement, T_g :

- a. $\varepsilon_g \leq 0.05$ using the long-term geosynthetic reinforcement stiffness, J_g
- b. $T_g \leq$ the allowable long-term geosynthetic tensile strength of the combined layers of geosynthetic reinforcement

Appropriate reduction factors for installation damage, creep, and degradation should be applied to obtain the long-term strength (see Koerner 2005).

8. Calculate the average embankment settlement, S , as the sum of the embankment compliance, S_E , the compression of the columns, S_C , and the compression of underlying material, S_U , if significant. The sum of S_E and S_C is calculated in the workbook. The value of S_U can be determined using the approach of Broms (1991), in which the embankment load is transferred to the bottom of the columns and the load is distributed with depth using a 1H:2V load spread below the bottom of the columns. The embankment settlement, S , determined this way represents the average settlement of the pavement surface. The differential settlement of the pavement surface should be small if the criteria and details in steps 3 and 4 are properly addressed.

If a significant time period elapses between the mid-point of embankment construction and pavement placement, Janbu's (1963) method can be used to estimate the portion of the embankment settlement that occurs before the pavement is constructed. The GeogridBridge workbook computes this settlement and subtracts it from the total embankment settlement to obtain the post-construction settlement of the pavement.

9. If the embankment settlement is too large, the design process should be repeated using a closer column spacing, a larger area replacement ratio, stiffer geosynthetic reinforcement, stiffer columns, and/or a preload.
10. Develop the geosynthetic details:
 - a. The bottom layer of geosynthetic should be placed on a lift of compacted bridging layer material at an elevation 6 in. above the top of the columns or pile caps.
 - b. Each additional layer of geosynthetic, if used, should be separated from the underlying layer of geosynthetic by a 6 in. lift of compacted bridging layer material.
 - c. Adjacent sheets of geosynthetic reinforcement should be overlapped sufficiently to transfer tension from one sheet to the next. According to Kempfert et al. (2004), adjacent sheets should overlap by a distance equal to the column diameter, and the overlaps should be located above the columns.

Example 1

The following example demonstrates the above design procedure, following the step-by-step sequence described above.

1. The embankment will be 8 ft high with a pavement and traffic surcharge of 300 psf. The post-construction embankment settlement is to be limited to 2 inches. The pavement will be placed 60 days after embankment construction.
2. The subsurface conditions are shown in Figure 12. The material property values are obtained from field and laboratory data with an appropriate degree of conservatism. When the embankment plus surcharge load is applied to the foundation profile in Figure 12 without any improvement, the calculated settlement for a wide embankment is 24 in., which greatly exceeds the allowable settlement of 2 in.
3. Columns installed by the deep-mixing method are being considered for this project. A diameter, d_c , of 3 ft and a center-to-center spacing, s , of 7 ft are selected for trial. These dimensions satisfy the criteria provided above, as follows with $a = 0.886d_c = 2.66$ ft:
 - a. $s - a = 4.34 \text{ ft} \leq H = 8 \text{ ft}$
 - b. $s - a = 4.34 \text{ ft} \leq 8 \text{ ft}$
 - c. $a_s = 0.144 \geq 0.1$
4. A GW sand and gravel is locally available for use in the bridging layer. The property values of the compacted sand and gravel are estimated to be: $\gamma = 135$ pcf, $\phi = 38$ degrees, $E = 750,000$ psf, $\nu = 0.3$. Because 3 ft of loose sand exists as the uppermost foundation soil at the site, it is judged that a value of $H_{b,red}$ equal to 1.0 ft can be safely applied. A bridging layer thickness, H_b , equal to 3.5 ft is selected, which satisfies the thickness requirement because it exceeds the maximum of 3 ft and $s - a - H_{b,red} = 3.3$ ft.
5. An MH sandy silt is locally available for use above the bridging layer. The properties of the compacted sandy silt are estimated to be as follows: $\gamma = 115$ pcf, $\phi = 30$ degrees, $E = 300,000$ psf, $\nu = 0.33$. The thickness of the sandy silt will be 4.5 ft to make up the total embankment height of 8 ft.
6. The columns are designed to be able to carry the full embankment and surcharge load within the area of a unit cell: $[(135 \text{ pcf})(3.5 \text{ ft}) + (115 \text{ pcf})(4.5 \text{ ft}) + 300 \text{ psf}](7 \text{ ft})^2 = 63,000$ lb. This requires that the design value of the unconfined compressive strength, q_u , of the columns should exceed $1.1(\gamma H + q)/a_s$, which is equal to 68 psi for the conditions of this example, by a suitable factor of safety. A design value of q_u equal to 150 psi was selected, and this provides a safety factor of 2.2 on the column strength. The value of E_{col} was estimated to be equal to $300q_u$, or 45,000 psi (6,500,000 psf), and $\nu_{col} = 0.30$.
7. Two layers of geosynthetic with a combined long-term stiffness of 48,000 lb/ft and a combined long-term allowable tensile strength of 2,000 lb/ft are selected for trial in the GeogridBridge workbook, whose results are shown in Figure 13. It can be seen that the calculated value of geosynthetic strain is 0.039 and geosynthetic tension is 1,870 lb/ft. Both values satisfy the design requirements.

8. The calculated value of post-construction embankment settlement is 1.8 inches. This satisfies the design requirement.
9. Since the design requirements are satisfied, further iterations are not needed.
10. The bottom layer of geosynthetic should be placed on a layer of compacted bridging layer material at a level 6 inches above the top of the columns, and the second layer of geosynthetic should be placed on another 6-in.-thick compacted lift of bridging layer material.

An additional analysis of this example was performed with the following change to the existing subsurface conditions: the upper layer of existing loose sand at the site is 6 ft thick instead of 3 ft thick, with the ground water level remaining at the top of the clay. In this case, it would be reasonable to judge that the value of $H_{b,red}$ can be set equal to 2.0 ft, based on the 6-ft-thickness of existing loose sand at the site. However, the required thickness of the bridging layer material is the maximum of 3 ft and $s - a - H_{b,red} = 4.34 - 2 = 2.34$ ft, so 3 ft controls as the required bridging layer thickness. The thickness of the overlying sandy silt is 5 ft to make up the total embankment height of 8 ft. The results from the GeogridBridge workbook analysis are shown in Figure 14, where it can be seen that the calculated values of geosynthetic strain and tension are 0.004 and 190 lb/ft, respectively. This 10-fold reduction in the geosynthetic strain and tension shows the important influence of the near-surface existing site conditions on system performance. In the case of the thicker layer of existing sand, geosynthetic reinforcement does not make a significant contribution to load transfer in the bridging layer, and the geosynthetic reinforcement can be removed from the design.

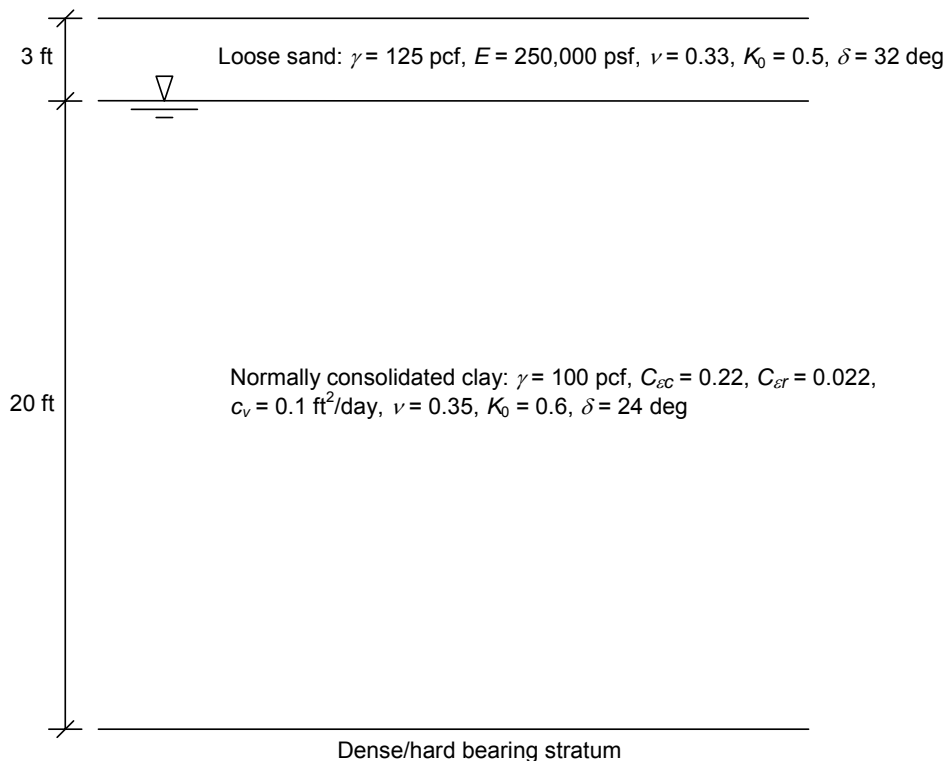


Figure 12. Subsurface profile for Example 1.

Example 1

	Bridging Layer Fill	Embankment Fill #2	Preload
Layer Thickness, H (ft)	3.5	4.5	0.0
Total Unit Weight, γ (pcf)	135	115	110
Friction Angle, ϕ (deg)	38	30	N/A
Young's Modulus, E (psf)	750,000	300,000	N/A
Poisson's Ratio, ν	0.30	0.33	N/A

Pavement plus Traffic Surcharge Pressure, q (psf)	300
---	-----

Time Available for Consolidation, t (days)	60
Allowable Post-Construction Settlement, S_A (in.)	2.0

Depth to Groundwater, d_w (ft)	3.0
Unit Weight of Groundwater, γ_w (pcf)	62.4

	Exist Sand #1	Exist Sand #2	Clay #1	Clay #2
Layer Thickness, H (ft)	3.0	0.0	20.0	0.0
Total Unit Weight, γ (pcf)	125	125	100	100
Young's Modulus, E (psf)	250,000	250,000	N/A	N/A
Poisson's Ratio, ν	0.33	0.30	0.35	0.35
Lat. Earth Press. Coeff., K_0	0.50	0.50	0.60	0.60
Interface Frict. Angle btwn Soil and Column, δ (deg)	32	32	24	24
Compression Ratio, $C_{\epsilon c}$	N/A	N/A	0.220	0.220
Recompression Ratio, $C_{\epsilon r}$	N/A	N/A	0.022	0.022
Coeff. of Consol., c_v (ft ² /day)	N/A	N/A	0.10	
Initial Eff. Vert. Stress at Top of Layer, $\sigma'_{v,top}$ (psf)	N/A	N/A	375	1127
Preconsol. Press. at Top of Layer, $p_{p,top}$ (psf)	N/A	N/A	375	1127
Initial Eff. Vert. Stress at Bottom of Layer, $\sigma'_{v,bot}$ (psf)	N/A	N/A	1127	1127
Preconsol. Press. At Bottom of Layer, $p_{p,bot}$ (psf)	N/A	N/A	1127	1127

Reduction in Required Bridging Layer Thickness, $H_{b,red}$ (ft)	1.0
--	-----

Geogrid Stiffness, J (lb/ft)	48,000
Long-term, In-Service, Allowable Geogrid Strength S_g (lb/ft)	2,000

	Pile Cap	Column
Vertical Distance from Top to Bottom of Element, H (ft)	0.0	23.0
Column Shape (use R for round and S for square)	R	R
Column Diameter or Width, d_c or a (ft)	3.0	3.0
Young's Modulus, E (psf)	6,500,000	6,500,000
Poisson's Ratio, ν	0.30	0.30
Center-to-center spacing, s (ft)	7.0	

	Value	Criterion
Clear Spacing, $s - a$ (ft)	4.3	≤ 8.0
Area Replacement Ratio at Ground Surface, a_s	0.144	≥ 0.10
Bridging Layer Thickness, H_b (ft)	3.5	≥ 3.3
Maximum differential settlement of geogrid, d (in.)	6.4	N/A
Geosynthetic Strain, ϵ_g	0.039	≤ 0.05
Tension in the Geosynthetic Reinforcement, T_g (lb/ft)	1,872	$\leq 2,000$
Post-Construction Embankment Settlement, S (in.)	1.8	≤ 2.0

Figure 13. Results from GeogridBridge workbook analysis of Example 1.

Example 1 with 6 ft of existing sand

	Bridging Layer Fill	Embankment Fill #2	Preload
Layer Thickness, H (ft)	3.0	5.0	0.0
Total Unit Weight, γ (pcf)	135	115	110
Friction Angle, ϕ (deg)	38	30	N/A
Young's Modulus, E (psf)	750,000	300,000	N/A
Poisson's Ratio, ν	0.30	0.33	N/A

Pavement plus Traffic Surcharge Pressure, q (psf)	300
---	-----

Time Available for Consolidation, t (days)	60
Allowable Post-Construction Settlement, S_A (in.)	2.0

Depth to Groundwater, d_w (ft)	6.0
Unit Weight of Groundwater, γ_w (pcf)	62.4

	Exist Sand #1	Exist Sand #2	Clay #1	Clay #2
Layer Thickness, H (ft)	6.0	0.0	20.0	0.0
Total Unit Weight, γ (pcf)	125	125	100	100
Young's Modulus, E (psf)	250,000	250,000	N/A	N/A
Poisson's Ratio, ν	0.33	0.30	0.35	0.35
Lat. Earth Press. Coeff., K_0	0.50	0.50	0.60	0.60
Interface Frict. Angle btwn Soil and Column, δ (deg)	32	32	24	24
Compression Ratio, $C_{\epsilon c}$	N/A	N/A	0.220	0.220
Recompression Ratio, $C_{\epsilon r}$	N/A	N/A	0.022	0.022
Coeff. of Consol., c_v (ft ² /day)	N/A	N/A	0.10	
Initial Eff. Vert. Stress at Top of Layer, $\sigma'_{v,top}$ (psf)	N/A	N/A	750	1502
Preconsol. Press. at Top of Layer, $p_{p,top}$ (psf)	N/A	N/A	750	1502
Initial Eff. Vert. Stress at Bottom of Layer, $\sigma'_{v,bot}$ (psf)	N/A	N/A	1502	1502
Preconsol. Press. At Bottom of Layer, $p_{p,bot}$ (psf)	N/A	N/A	1502	1502

Reduction in Required Bridging Layer Thickness, $H_{b,red}$ (ft)	2.0
--	-----

Geogrid Stiffness, J (lb/ft)	48,000
Long-term, In-Service, Allowable Geogrid Strength S_g (lb/ft)	2,000

	Pile Cap	Column
Vertical Distance from Top to Bottom of Element, H (ft)	0.0	26.0
Column Shape (use R for round and S for square)	R	R
Column Diameter or Width, d_c or a (ft)	3.0	3.0
Young's Modulus, E (psf)	6,500,000	6,500,000
Poisson's Ratio, ν	0.30	0.30
Center-to-center spacing, s (ft)	7.0	

	Value	Criterion
Clear Spacing, $s - a$ (ft)	4.3	≤ 8.0
Area Replacement Ratio at Ground Surface, a_s	0.144	≥ 0.10
Bridging Layer Thickness, H_b (ft)	3.0	≥ 3.0
Maximum differential settlement of geogrid, d (in.)	2.0	N/A
Geosynthetic Strain, ϵ_g	0.004	≤ 0.05
Tension in the Geosynthetic Reinforcement, T_g (lb/ft)	188	$\leq 2,000$
Post-Construction Embankment Settlement, S (in.)	0.7	≤ 2.0

Figure 14. Results from GeogridBridge workbook analysis of Example 1 with 6-ft-thick upper sand layer.

Example 2

The following example illustrates how to represent piles with pile caps in analysis of a pile-supported, geosynthetic-reinforced embankment.

1. The embankment will be 14 ft high with a pavement and traffic surcharge of 300 psf. The total embankment settlement is to be limited to 2 inches. The pavement will be placed 90 days after embankment construction.
2. The subsurface conditions are shown in Figure 15. The material property values are obtained from field and laboratory data with an appropriate degree of conservatism. When the embankment plus surcharge load is applied to the foundation profile in Figure 15 without any piles, the calculated settlement for a wide embankment is 41 in., which greatly exceeds the allowable settlement of 2 in.
3. A pile cap width, a , of 4 ft and a center-to-center spacing, s , of 11 ft are selected for trial. These dimensions satisfy the criteria described above:
 - a. $s - a = 7 \text{ ft} \leq H = 14 \text{ ft}$
 - b. $s - a = 7 \text{ ft} \leq 8 \text{ ft}$
 - c. $a_s = 0.132 \geq 0.1$
4. An SW sand is locally available for use in the bridging layer. The properties of the compacted sand are estimated to be as follows: $\gamma = 130 \text{ pcf}$, $\phi = 36 \text{ degrees}$, $E = 600,000 \text{ psf}$, $\nu = 0.3$. Because 5 ft of medium dense sand exists as the uppermost foundation soil at the site, it is judged that a value of $H_{b,red}$ equal to 2.5 ft can be safely applied. A bridging layer thickness, H_b , equal to 4.5 ft is selected, which satisfies the thickness requirement because it equals the maximum of 3 ft and $s - a - H_{b,red} = 4.5 \text{ ft}$.
5. An MH sandy silt is locally available for use above the bridging layer. The properties of the compacted sandy silt are estimated to be as follows: $\gamma = 115 \text{ pcf}$, $\phi = 32 \text{ degrees}$, $E = 300,000 \text{ psf}$, $\nu = 0.33$. The thickness of the compacted sandy silt will be 9.5 ft to make up the total embankment height of 14 ft.
6. The piles are designed to be able to carry the full embankment and surcharge load within the area of a unit cell: $[(130 \text{ pcf})(4.5 \text{ ft}) + (115 \text{ pcf})(9.5 \text{ ft}) + 300 \text{ psf}](11 \text{ ft})^2 = 240,000 \text{ lb}$. Square, 24-in. by 24-in., prestressed concrete piles are selected to support this load. Values of E and ν equal to 4,000 ksi (580,000,000 psf) and 0.2, respectively, are selected for the pile. The same property values are assigned to the pile cap, which is 2 feet thick.
7. Three layers of geosynthetic with a combined long-term stiffness of 72,000 lb/ft and a combined long-term allowable tensile strength of 3,000 lb/ft are selected for trial in the GeogridBridge workbook, whose results are shown in Figure 16. It can be seen that the calculated value of geosynthetic strain is 0.032 and the calculated value of geosynthetic tension is 2,300 lb/ft. Both values satisfy the design requirements.

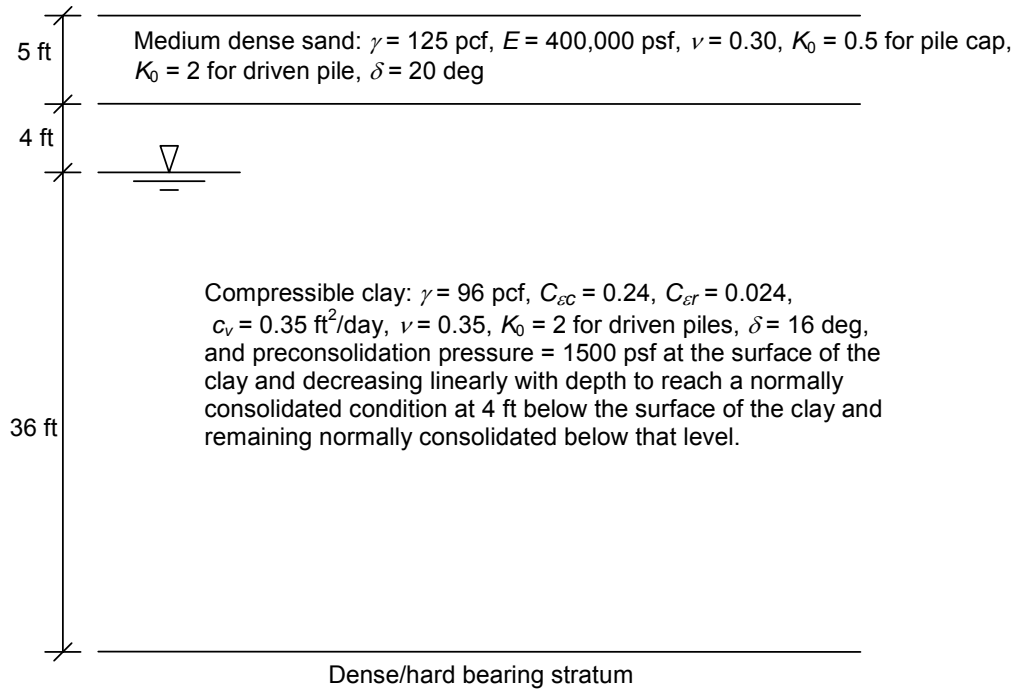


Figure 15. Subsurface profile for Example 2.

8. The calculated value of post-construction embankment settlement is 2.0 inches. This satisfies the design requirement.
9. Since the design requirements are satisfied, further iterations are not needed.
10. The bottom layer of geosynthetic should be placed on a layer of compacted bridging layer material at a level 6 inches above the top of the columns, and the second and third layers of geosynthetic should each be placed on additional 6-in.-thick layers of compacted bridging layer material.

An additional analysis of this example was performed with only a 2-ft-thick upper layer of existing sand. In this case, the value of $H_{b,red}$ is set equal to 1.0 ft, and the required thickness of the bridging layer material is the maximum of 3 ft and $s - a - H_{b,red} = 11 - 4 - 1 = 6$ ft, so the bridging layer thickness is set equal to 6 ft, and the thickness of the overlying sandy silt is 8 ft to make up the total embankment height of 14 ft. The results from the GeogridBridge analysis are shown in Figure 17, where it can be seen that a combined geogrid stiffness and strength of 216,000 lb/ft and 9,000 lb/ft, respectively, provide sufficient capacity to satisfy the strain and tensile strength criteria, but the post-construction settlement criterion of 2.0 in. is slightly exceeded by the calculated value of 2.1 in. This outcome represents a 3-fold increase in the requirements for geogrid reinforcing, which again shows the important influence of subsurface conditions on system performance.

In situations like this one, the designer could evaluate a larger pile cap width to reduce the demand on the geogrid. Example 2 was analyzed once again with the 2-ft-thick upper sand layer, but with a 5-ft-wide pile cap. Maintaining a value of $H_{b,red}$ equal to 1.0 ft, the required bridging layer thickness is the maximum of 3 ft and $s - a - H_{b,red} = 11 - 5 - 1 = 5$ ft, so the

Example 2

	Bridging Layer Fill	Embankment Fill #2	Preload
Layer Thickness, H (ft)	4.5	9.5	0.0
Total Unit Weight, γ (pcf)	130	115	110
Friction Angle, ϕ (deg)	36	32	N/A
Young's Modulus, E (psf)	600,000	300,000	N/A
Poisson's Ratio, ν	0.30	0.33	N/A

Pavement plus Traffic Surcharge Pressure, q (psf)	300
---	-----

Time Available for Consolidation, t (days)	90
Allowable Post-Construction Settlement, S_A (in.)	2.0

Depth to Groundwater, d_w (ft)	9.0
Unit Weight of Groundwater, γ_w (pcf)	62.4

	Exist Sand #1	Exist Sand #2	Clay #1	Clay #2
Layer Thickness, H (ft)	2.0	3.0	4.0	36.0
Total Unit Weight, γ (pcf)	125	125	96	96
Young's Modulus, E (psf)	400,000	400,000	N/A	N/A
Poisson's Ratio, ν	0.30	0.30	0.35	0.35
Lat. Earth Press. Coeff., K_0	0.50	2.00	2.00	2.00
Interface Frict. Angle btwn Soil and Column, δ (deg)	20	20	16	16
Compression Ratio, $C_{\epsilon c}$	N/A	N/A	0.240	0.240
Recompression Ratio, $C_{\epsilon r}$	N/A	N/A	0.024	0.024
Coeff. of Consol., c_v (ft ² /day)	N/A	N/A	0.35	
Initial Eff. Vert. Stress at Top of Layer, $\sigma'_{v,top}$ (psf)	N/A	N/A	625	1009
Preconsol. Press. at Top of Layer, $p_{p,top}$ (psf)	N/A	N/A	1500	1009
Initial Eff. Vert. Stress at Bottom of Layer, $\sigma'_{v,bot}$ (psf)	N/A	N/A	1009	2219
Preconsol. Press. At Bottom of Layer, $p_{p,bot}$ (psf)	N/A	N/A	1009	2219

Reduction in Required Bridging Layer Thickness, $H_{b,red}$ (ft)	2.5
--	-----

Geogrid Stiffness, J (lb/ft)	72,000
Long-term, In-Service, Allowable Geogrid Strength S_g (lb/ft)	3,000

	Pile Cap	Column
Vertical Distance from Top to Bottom of Element, H (ft)	2.0	43.0
Column Shape (use R for round and S for square)	S	S
Column Diameter or Width, d_c or a (ft)	4.0	2.0
Young's Modulus, E (psf)	580,000,000	580,000,000
Poisson's Ratio, ν	0.20	0.20
Center-to-center spacing, s (ft)	11.0	

	Value	Criterion
Clear Spacing, $s - a$ (ft)	7.0	≤ 8.0
Area Replacement Ratio at Ground Surface, a_s	0.132	≥ 0.10
Bridging Layer Thickness, H_b (ft)	4.5	≥ 4.5
Maximum differential settlement of geogrid, d (in.)	9.4	N/A
Geosynthetic Strain, ϵ_g	0.032	≤ 0.05
Tension in the Geosynthetic Reinforcement, T_g (lb/ft)	2,297	$\leq 3,000$
Post-Construction Embankment Settlement, S (in.)	2.0	≤ 2.0

Figure 16. Results from GeogridBridge workbook analysis of Example 2.

Example 2 with 2-ft-thick upper sand layer

	Bridging Layer Fill	Embankment Fill #2	Preload
Layer Thickness, H (ft)	6.0	8.0	0.0
Total Unit Weight, γ (pcf)	130	115	110
Friction Angle, ϕ (deg)	36	32	N/A
Young's Modulus, E (psf)	600,000	300,000	N/A
Poisson's Ratio, ν	0.30	0.33	N/A

Pavement plus Traffic Surcharge Pressure, q (psf)	300
---	-----

Time Available for Consolidation, t (days)	90
Allowable Post-Construction Settlement, S_A (in.)	2.0

Depth to Groundwater, d_w (ft)	6.0
Unit Weight of Groundwater, γ_w (pcf)	62.4

	Exist Sand #1	Exist Sand #2	Clay #1	Clay #2
Layer Thickness, H (ft)	2.0	0.0	4.0	36.0
Total Unit Weight, γ (pcf)	125	125	96	96
Young's Modulus, E (psf)	400,000	400,000	N/A	N/A
Poisson's Ratio, ν	0.30	0.30	0.35	0.35
Lat. Earth Press. Coeff., K_0	0.50	2.00	2.00	2.00
Interface Frict. Angle btwn Soil and Column, δ (deg)	20	20	16	16
Compression Ratio, $C_{\epsilon c}$	N/A	N/A	0.240	0.240
Recompression Ratio, $C_{\epsilon r}$	N/A	N/A	0.024	0.024
Coeff. of Consol., c_v (ft ² /day)	N/A	N/A	0.35	
Initial Eff. Vert. Stress at Top of Layer, $\sigma'_{v,top}$ (psf)	N/A	N/A	250	634
Preconsol. Press. at Top of Layer, $p_{p,top}$ (psf)	N/A	N/A	1500	634
Initial Eff. Vert. Stress at Bottom of Layer, $\sigma'_{v,bot}$ (psf)	N/A	N/A	634	1844
Preconsol. Press. At Bottom of Layer, $p_{p,bot}$ (psf)	N/A	N/A	634	1844

Reduction in Required Bridging Layer Thickness, $H_{b,red}$ (ft)	1.0
--	-----

Geogrid Stiffness, J (lb/ft)	216,000
Long-term, In-Service, Allowable Geogrid Strength S_g (lb/ft)	9,000

	Pile Cap	Column
Vertical Distance from Top to Bottom of Element, H (ft)	2.0	40.0
Column Shape (use R for round and S for square)	S	S
Column Diameter or Width, d_c or a (ft)	4.0	2.0
Young's Modulus, E (psf)	580,000,000	580,000,000
Poisson's Ratio, ν	0.20	0.20
Center-to-center spacing, s (ft)	11.0	

	Value	Criterion
Clear Spacing, $s - a$ (ft)	7.0	≤ 8.0
Area Replacement Ratio at Ground Surface, a_s	0.132	≥ 0.10
Bridging Layer Thickness, H_b (ft)	6.0	≥ 6.0
Maximum differential settlement of geogrid, d (in.)	9.9	N/A
Geosynthetic Strain, ϵ_g	0.036	≤ 0.05
Tension in the Geosynthetic Reinforcement, T_g (lb/ft)	7,775	$\leq 9,000$
Post-Construction Embankment Settlement, S (in.)	2.1	≤ 2.0

Figure 17. Results from GeogridBridge workbook analysis of Example 2 with 2-ft-thick upper sand layer.

Example 2 with 2-ft-thick upper sand layer and 5-ft-wide pile caps

	Bridging Layer Fill	Embankment Fill #2	Preload	
Layer Thickness, H (ft)	5.0	9.0	0.0	
Total Unit Weight, γ (pcf)	130	115	110	
Friction Angle, ϕ (deg)	36	32	N/A	
Young's Modulus, E (psf)	600,000	300,000	N/A	
Poisson's Ratio, ν	0.30	0.33	N/A	

Pavement plus Traffic Surcharge Pressure, q (psf)	300
---	-----

Time Available for Consolidation, t (days)	90
Allowable Post-Construction Settlement, S_A (in.)	2.0

Depth to Groundwater, d_w (ft)	6.0
Unit Weight of Groundwater, γ_w (pcf)	62.4

	Exist Sand #1	Exist Sand #2	Clay #1	Clay #2
Layer Thickness, H (ft)	2.0	0.0	4.0	36.0
Total Unit Weight, γ (pcf)	125	125	96	96
Young's Modulus, E (psf)	400,000	400,000	N/A	N/A
Poisson's Ratio, ν	0.30	0.30	0.35	0.35
Lat. Earth Press. Coeff., K_0	0.50	2.00	2.00	2.00
Interface Frict. Angle btwn Soil and Column, δ (deg)	20	20	16	16
Compression Ratio, $C_{\epsilon c}$	N/A	N/A	0.240	0.240
Recompression Ratio, $C_{\epsilon r}$	N/A	N/A	0.024	0.024
Coeff. of Consol., c_v (ft ² /day)	N/A	N/A	0.35	
Initial Eff. Vert. Stress at Top of Layer, $\sigma'_{v,top}$ (psf)	N/A	N/A	250	634
Preconsol. Press. at Top of Layer, $p_{p,top}$ (psf)	N/A	N/A	1500	634
Initial Eff. Vert. Stress at Bottom of Layer, $\sigma'_{v,bot}$ (psf)	N/A	N/A	634	1844
Preconsol. Press. At Bottom of Layer, $p_{p,bot}$ (psf)	N/A	N/A	634	1844

Reduction in Required Bridging Layer Thickness, $H_{b,red}$ (ft)	1.0
--	-----

Geogrid Stiffness, J (lb/ft)	72,000
Long-term, In-Service, Allowable Geogrid Strength S_g (lb/ft)	3,000

	Pile Cap	Column
Vertical Distance from Top to Bottom of Element, H (ft)	2.0	40.0
Column Shape (use R for round and S for square)	S	S
Column Diameter or Width, d_c or a (ft)	5.0	2.0
Young's Modulus, E (psf)	580,000,000	580,000,000
Poisson's Ratio, ν	0.20	0.20
Center-to-center spacing, s (ft)	11.0	

	Value	Criterion
Clear Spacing, $s - a$ (ft)	6.0	≤ 8.0
Area Replacement Ratio at Ground Surface, a_s	0.207	≥ 0.10
Bridging Layer Thickness, H_b (ft)	5.0	≥ 5.0
Maximum differential settlement of geogrid, d (in.)	9.2	N/A
Geosynthetic Strain, ϵ_g	0.040	≤ 0.05
Tension in the Geosynthetic Reinforcement, T_g (lb/ft)	2,908	$\leq 3,000$
Post-Construction Embankment Settlement, S (in.)	1.8	≤ 2.0

Figure 18. Results from GeogridBridge workbook analysis of Example 2 with 2-ft-thick upper sand layer and with 5-ft-wide pile caps.

bridging layer thickness is set equal to 5 ft. The thickness of the overlying sandy silt is 9 ft to make up the total embankment height of 14 ft. The results from a GeogridBridge analysis of this case are presented in Figure 18, which shows that all design requirements are satisfied by the wider pile cap combined with the original combined geogrid stiffness and strength of 72,000 lb/ft and 3,000 lb/ft, respectively. Using 5-ft-wide pile caps at an 11-ft center-to-center spacing produces an area replacement ratio of 21%.

DISCUSSION

This section presents discussion of the results from the literature review, the numerical stress-strain analyses, and development of the analysis and design procedures.

Literature Review

There is general agreement in the literature regarding suitable procedures for estimating compression of ground improved or reinforced with piles or other columns, as well for estimating the compression of ground underneath the columns.

Regarding the component of settlement due to embankment compliance, Russell et al. (2003) acknowledge that their procedure is approximate. Refinements in this procedure based on careful numerical analyses and field measurements would be beneficial. Such analyses could also be used to develop a rational procedure for relating differential settlements at the base of the embankment to differential settlements at the ground surface. At present, differential settlements at the embankment surface are controlled to a large extent by using rules of thumb relating maximum column spacing to embankment height.

There is not widespread agreement in the literature regarding methods to calculate the limiting value of vertical load that embankments apply to geosynthetic reinforcement in column-supported embankments. However, it is the authors' opinion that the Adapted Terzaghi Method (Russell and Pierpoint 1997), the Hewlett and Randolph Method (1988), and the Kempfert et al. (2004) Method show the most promise because they are based on principles of mechanics and have been verified by tests and analyses. Neither the BS8006 (1995) method nor the Adapted Guido Method (Russell and Pierpoint 1997) appears to the authors to be suitable for the purpose of determining the limiting value of vertical load acting on geosynthetic reinforcement.

Most methods presented in the literature for calculating the strain and tension that develop in geosynthetic reinforcement in column-supported embankments are similar to the method presented in BS8006 (1995). An important exception is the method developed by Kempfert et al. (2004), which is based on a theory of an elastic embedded membrane. For the same vertical load, geometry, and geosynthetic stiffness, the Kempfert et al. (2004) method produces higher strains in the geosynthetic than does the BS8006 (1995) method. The BS8006 (1995) method for calculating the strain and tension in geosynthetic reinforcement was adopted in the procedure recommended in this report. Further measurements and analyses are warranted to determine which method best reflects performance in practice.

There are some variations in recommendations in the literature regarding system details, such as limiting column spacing versus embankment height, positioning of reinforcement layers, and quality and thickness of bridging layer fill. The approaches adopted here follow the dominate usage found in the literature.

Numerical Analyses

The numerical analyses employed in this research were verified against closed-form solutions, pilot-scale tests, and case histories. The verified numerical methods were used in a parameter study that showed (1) logical increases in SRR_{net} values with increases in clear spacing between columns and increasing geosynthetic stiffness and (2) logical decreases in SRR_{net} values with increasing stiffness and strength of the foundation and embankment soils and with increasing elevation of the geosynthetic above the top of the columns or pile caps

The verified numerical analysis procedures were applied to a range of system parameter variations, and the results were used to validate the simplified computational model for SRR_{net} that was developed and implemented in a Microsoft Excel® workbook.

Analysis and Design Procedures

Simplified procedures were developed for analysis and design of column-supported, geosynthetic-reinforced embankments based on results of the literature review and the numerical analyses. The analysis procedures are for settlement and load transfer, but not for embankment stability, which will be addressed in a later report. The analysis procedures were implemented in a workbook that permits substantial flexibility in embankment conditions, foundation conditions, and column type. The columns can be driven piles with pile caps, vibro-concrete columns, or other types of columns. The workbook is easy to use, and it solves the nonlinear simultaneous equations that yield values of strain in the geosynthetic, tension in the geosynthetic, and embankment settlement.

The design procedures that were developed around the simplified computational model incorporate features of practice that have been reported in the literature for column-supported, geosynthetic-reinforced embankments.

Both the numerical analyses and the simplified analysis procedure demonstrate the important impact that subgrade support has on the net vertical loads that are applied to geosynthetic reinforcement. If the subgrade support is good, like that provided by a layer of medium dense sand or stiff clay, and if the clear spacing between columns or pile caps is not too large, geosynthetic reinforcement does not have a significant effect on system performance. If the subgrade support is poor, like that provided by normally consolidated clay or peat, and if the clear spacing between columns or pile caps is large, it can become difficult to provide enough geosynthetic reinforcement to support the applied loads and limit deformations to acceptable magnitudes. In such cases, it may be necessary to reduce the clear spacing between columns or pile caps. For appropriate column spacings and subgrade support conditions, geosynthetic reinforcement can enhance system performance.

CONCLUSIONS

Although the literature exhibits substantial agreement among many aspects of design of column-supported, geosynthetic-reinforced embankments, there is disagreement among methods to determine the magnitude of vertical load that acts on the geosynthetic reinforcement in these systems. A key finding of this research is that a mechanistically based method, such as the Adapted Terzaghi Method (Russell and Pierpoint 1998), can be used in combination with the stiffnesses of the embankment, geosynthetic, and the foundation system to rationally evaluate the net load on the geosynthetic reinforcement. The net load can then be used to rationally evaluate the strain and tension in the geosynthetic.

RECOMMENDATIONS

1. VDOT's geotechnical engineers should use the procedures described in this report to design column-supported, geosynthetic-reinforced embankments based on considerations of settlement and load-transfer in bridging layers.
2. The Virginia Transportation Research Council should further improve the state of practice by completing research on the following:
 - An improved method should be developed to relate embankment compliance at subgrade level to total and differential settlement of the embankment surface.
 - Additional three-dimensional numerical analyses should be performed to further investigate strain and tension in the geosynthetic reinforcement. In such analyses, consideration should be given to all aspects of system geometry, including the use of multiple layers of geosynthetic reinforcement and the influence of the plan view orientation and vertical position of the reinforcement on its effectiveness in transferring embankment loads to the columns.

COSTS AND BENEFITS ASSESSMENT

Because the purpose of this research is to develop analysis and design methods for column-supported embankments, assessment of the costs and benefits of the methods must be on a qualitative basis. The costs include the time to study, learn, and use the new methods. Another potential cost is that there is risk associated with using new methods. However, this risk is judged to be low because the new methods have been verifying against numerical analyses, and the numerical analysis procedures were verified against closed-form solutions, pilot-scale tests, and field case histories. Furthermore, any risk associated with applying the new methods can be minimized by assuming appropriately conservative material property values. A designer can be as conservative as he or she wants by simply choosing low values of strength and stiffness for the embankment and foundation soils.

The major benefits of the new methods arise from the same issues described in the preceding paragraph as producing costs. Because the new methods are logical and implemented in an easy-to-use workbook, they are easy to learn and apply. Because the new methods make use of well established existing methods for column-supported embankments combined with other well established methods from geotechnical engineering, and because extensive numerical verification studies have been performed, the designer can have confidence that a mechanistically sound and comprehensive procedure has been developed. As with all geotechnical engineering design procedures, this one should be applied with sound judgment and careful evaluation of project-specific details, including subsurface conditions, construction methods, contracting practices, loading conditions, and performance requirements.

ACKNOWLEDGMENTS

Funding for this research was provided by the Virginia Transportation Research Council, the National Deep Mixing Program, the National Science Foundation, and Virginia Tech. The authors recognize the important contributions made by Jie Han, Stanley Hite, Edward Hoppe, Jose Gomez III, Meeok Kim, Michael McGuire, Michael Navin, Patrick Naughton, Silas Nichols, Thomas Pelnik, Ali Porbaha, Jen Schaeffer, David Shiells, and Masaaki Terashi.

REFERENCES

- Barksdale, R. D., and Bachus, R. C. *Design and construction of stone columns, Volume 1*. Report No. FHWA-RD-83-026, Federal Highway Administration, McLean, Virginia, 1983.
- Bell, A. L., Jenner, C., Maddison, J. D., and Vignoles, J. Embankment support using geogrids with vibro concrete columns. *Proceedings, 5th International Conference on Geotextiles, Geomembranes, and Related Products*, Vol. 1, Karunaratne, Chew and Wong (eds), Singapore, September 1994, pp. 335-338.
- Bentler, D.J., Morrison, C.S., Esterhuizen, J.J.B., and Duncan, J.M. *SAGE User's Guide: A Finite Element Program for Static Analysis of Geotechnical Engineering Programs*, Center for Geotechnical Practice and Research, Virginia Tech, Blacksburg, Virginia, 1999.
- British Standards Institution. BS8006 Code of Practice for Strengthened/Reinforced Soils and Other Fills. London, U.K, 1995.
- Broms, B. B. Keynote Lecture: Design of lime, lime/cement and cement columns. *International Conference on Dry Mix Methods: Dry Mix Methods for Deep Soil Stabilization*, Bredenberg, Holm, & Broms (eds), Balkema, Rotterdam, 1999, pp. 125-153.
- Broms, B. B. Stabilization of Soil with Lime Columns. *Foundation Engineering Handbook*, Chapter 24, Second Edition, van Nostrand Reinhold, New York, 1991, pp. 833-855.

- Carlsten, P., and Ekstrom, J. *Lime and Lime/Cement Columns*. Swedish Geotechnical Society Report 4:95E, Linköping, Sweden, 1995.
- Card, G. B., and Carter, G.R. Case history of a piled embankment in London's Docklands. *Engineering Geology of Construction*, Geological Society Engineering Geology Special Publication No. 10, Edleston, M., Walthall, S., Cripps, J.C. and Culshaw, M.G. (eds.), 1995, pp. 79-84.
- CDIT (Coastal Development Institute of Technology). *The Deep Mixing Method: Principle, Design and Construction*. A.A. Balkema, The Netherlands, 2002.
- Collin, J. G. Column supported embankment design considerations. *Proceedings of the 52nd Annual Geotechnical Engineering Conference*, J.F. Labuz and J.G. Bentler (eds.), Minnesota, February 2004, pp. 51-78.
- EuroSoilStab. *Development of design and construction methods to stabilise soft organic soils*. Design Guide Soft Soil Stabilization, CT97-0351 Project No.: BE 96-3177, European Commission, Bryssel, 2002.
- Guido, V. A., Knueppel, J.D. and Sweeny, M.A. Plate loading tests on geogrid-reinforced earth slabs. *Geosynthetic '87 Conference*, New Orleans, 1987, pp. 216-225.
- Habib, H. A. A., Brugman, M.H.A. and Uijting, B.G.J. Widening of Road N247 founded on a geogrid reinforced mattress on piles. *Proceedings, 7th International Conference on Geosynthetics*, Delmas, Gourc, & Girard (eds), Swets & Zeitlinger, Lisse, September 2002, pp. 369-372.
- Han, J., and Gabr, M.A. Numerical analysis of geosynthetic-reinforced and pile-supported earth platforms over soft soil. *Journal of Geotechnical and Geoenvironmental Engineering*, Vol. 128, No. 1, January 2002, pp. 44-53.
- Hannigan, P. J., Goble, G. G., Thendean, G., Likins, G. E., and Raushe, F., *Design and Construction of Driven Pile Foundations*, Report No. FHWA-HI-97-013, Federal Highway Administration, Washington, DC, January 1997
- Hewlett, W. J., and Randolph, M.F. Analysis of piled embankments. *Ground Engineering*, Vol. 22, No. 3, April 1988, pp. 12-18.
- Horgan, G. J., and Sarsby, R.W. The arching effect of soils over voids and piles incorporating geosynthetic reinforcement. *Proceedings, 7th International Conference on Geosynthetics*, Delmas, Gourc, & Girard (eds), Swets & Zeitlinger, Lisse, September 2002, pp. 373-378.
- ITASCA Consulting Group. *FLAC Fast Lagrangian Analysis of Continua*, ITASCA Consulting Group, Minneapolis, Minnesota, 2002a.
- ITASCA Consulting Group. *FLAC3D Fast Lagrangian Analysis of Continua in 3 Dimensions*, ITASCA Consulting Group, Minneapolis, Minnesota, 2002b.

- Jenner, C. G., Austin, R.A. and Buckland, D. Embankment support over piles using geogrids. *Proceedings of 6th International Conference on Geosynthetics*, Vol. 1, Rowe, R.K. (ed.), Atlanta, Georgia, March 1998, pp. 763-766.
- John, N. W. M. *Geotextiles*. Blackie & Son Ltd., Glasgow and London, 1987.
- Jones, C. J. F. P., Lawson, C.R., and Ayres, D.J. Geotextile reinforced piled embankments. *Proceedings, 4th International Conference on Geotextiles, Geomembranes, and Related Products*, Vol. 1, G. Den Hoedt (ed), The Hague, May - June 1990, pp. 155-160.
- Kempfert, H.-G., Gobel, C., Alexiew, D. and Heitz, C. German recommendations for reinforced embankments on pile-similar elements. *EuroGeo3 - Third European Geosynthetics Conference, Geotechnical Engineering with Geosynthetics*, 2004, pp. 279-284.
- Kempfert, H. - G., Stadel, M. and Zaeske, D. Design of geosynthetic-reinforced bearing layers over piles. *Bautechnik*, Vol. 74, No. 12, December 1997, pp. 818-825.
- Koerner, R. M. *Designing with Geosynthetics*, 5th ed., Prentice Hall, Upper Saddle River, New Jersey, 2005.
- Kempton, G., Russell, D., Pierpoint, N.D. and Jones, C. J. F. P. Two- and three-dimensional numerical analysis of the performance of piled embankments. *Proceedings, 6th International Conference on Geosynthetics*, Vol. 2, Rowe, R.K. (ed.), Atlanta, Georgia, March 1998, pp. 767-772.
- Lawson, C. R. Soil reinforcement with geosynthetics. *Applied Ground Improvement Techniques*, Southeast Asian Geotechnical Society (SEAGS), December 1992, pp. 55-74.
- Love, J., and Milligan, G. Design methods for basally reinforced pile-supported embankments over soft ground. *Ground Engineering*, Vol. 36, No. 3, March 2003, pp. 39-43.
- Morrison, C. S., Duncan, J. M., Filz, G. M., Robbins, D. H., and Reddy, J. N. *SAGE: A Finite Element Computer Program for Static Analyses of Geotechnical Engineering Problems*, The Charles E. Via Department of Civil Engineering, Virginia Tech, Blacksburg, Virginia, 1993.
- O'Neill, M. W., and Reese, L. C. *Drilled Shafts: Construction Procedures and Design Methods*, ADSC-TL-4, FHWA-IF-99-025, Federal Highway Administration, Washington, DC, 1999.
- Poulos, H. GC and Davis, E. H. *Elastic Solutions for Soil and Rock Mechanics*, John Wiley & Sons, Inc., New York , 1974
- Priebe, H. J. The design of vibro replacement. *Ground Engineering*, Vol. 28, No. 10, December 1995, pp. 31-37.

- Rogbeck, Y., Gustavsson, S., Sodergren, I., and Lindquist, D. Reinforced piled embankments in Sweden - design aspects. *Proceedings, Sixth International Conference on Geosynthetics*, Vol. 2, Rowe, R.K. (ed.), Atlanta, Georgia, March 1998, pp. 755-762.
- Russell, D., Naughton, P.J. and G. Kempton, G. A new design procedure for piled embankments. *Proceedings of the 56th Canadian Geotechnical Conference and 2003 NAGS Conference*, Vol. 1, Winnipeg, MB, September – October 2003, pp. 858-865.
- Russell, D., and Pierpoint, N. An assessment of design methods for piled embankments. *Ground Engineering*, Vol. 30, No. 11, November 1997, pp. 39-44.
- Smith, M. E. Design of Bridging Layers in Geosynthetic-Reinforced Column-Supported Embankments, Doctoral Dissertation, Virginia Tech, Blacksburg, Virginia, 2005.
- Stewart, M. E., Navin, M.P., and Filz, G.M. Analysis of a column-supported test embankment at the I-95/Route 1 interchange. *Proceedings of Geo-Trans 2004, Geotechnical Engineering for Transportation Projects, Geotechnical Special Publication No. 126*, ASCE, 2004, pp. 1337-1346.
- Ugural, A.C. *Stresses in plates and shells*. McGraw Hill, New York, 1999.